Geophys. J. Int. (1992) **108,** 812–832

A seismic refraction investigation of the Archaean Kaapvaal Craton, South Africa, using mine tremors as the energy source

R. J. Durrheim[1] and R. W. E. Green[2]

[1]*Department of Geophysics, University of the Witwatersrand, Private Bag 3, WITS 2050, South Africa*
[2]*Bernard Price Institute for Geophysical Research, University of the Witwatersrand, Private Bag 3, WITS 2050, South Africa*

Accepted 1991 September 16. Received 1991 September 16; in original form 1991 March 25

SUMMARY

The structure of the central Kaapvaal Craton of southern Africa has been investigated by deep seismic sounding, using mine tremors as energy sources. Seismometers were deployed at approximately 10 km intervals on two profiles stretching between major mine tremor source regions. Mine tremors are rich in shear energy enabling joint interpretation of *P*- and *S*-waves and produce substantial energy at frequencies as low as 1 Hz. Record sections are presented for both *P*- and *S*-waves, and the traveltimes and amplitudes interpreted using 2-D ray-tracing techniques. Synthetic seismograms computed for a 1-D velocity model by the reflectivity method compare well with the observed data. A generalized seismic model of the Kaapvaal Craton has the following features: supracrustal strata 0–10 km thick; upper crystalline basement with *P*-wave velocities of 6.0–6.2 km s^{-1}; the boundary between upper and lower crust at a depth of 14–18 km; a lower crust with a relatively uniform seismic velocity in the range 6.4–6.7 km s^{-1}; and the crust/mantle transition over 1–3 km with the Moho at a depth of about 35 km. The lower crust is found to be seismically attenuating and has a Poisson's ratio of about 0.28. It is also known to be electrically conductive. These observations are in accord with the presence of hydrated mantle rock at the base of the crust.

The velocity–depth model of the Kaapvaal Craton is similar to models derived for other Archaean cratons. The Proterozoic provinces adjacent to the Kaapvaal craton are significantly thicker, and have an intermediate- to high-velocity layer developed at the base of the crust. This is interpreted to indicate a change in the process of crustal growth, with basaltic underplating becoming more important since the Archaean. This change is attributed to a change in the composition of the upper mantle. The higher temperatures in the Archaean mantle led to the eruption of komatiitic lavas, resulting in an ultradepleted mantle unable to produce significant volumes of basaltic melt. Proterozoic crust developed above fertile mantle, and subsequent partial melting resulted in basaltic underplating and crustal inflation.

Key words: crustal structure, Kaapvaal Craton, seismic reflection.

INTRODUCTION

Seismic studies of the lithosphere provide critical information on its structure, composition and evolution. The Kaapvaal Craton of southern Africa has several characteristics which make it particularly suitable for the study of the Archaean continental lithosphere. The Craton has the world's greatest concentration of kimberlite intrusions. These diamond-bearing rocks have transported samples of the lower crust and upper mantle to the surface, providing insight into the composition of these regions. The Vredefort Dome, a cryptoexplosion structure some 40 km in diameter, is situated near the centre of the Craton. It is believed that the continental crust has been turned 'on edge' within the structure, providing a section through the entire crystalline crust. The xenoliths from kimberlites and the Vredefort crustal section provide constraints on the petrological interpretation of seismic velocities. The Craton hosts several major ore deposits, notably gold and uranium in the Witwatersrand Basin, and chromium and platinum group

metals in the Bushveld Complex. Consequently the geology of the Craton has been mapped in considerable detail. Lastly, deep-level mining for gold and uranium in the Witwatersrand Basin induces frequent earth tremors, providing a source of energy for deep seismic sounding.

During the 1950s several investigators utilized Witwatersrand mine tremors to study the seismic velocity structure of the Craton, deriving simple one- or two-layered models (Willmore, Hales & Gane 1952; Gane *et al.* 1956; Hales & Sacks 1959). Since the advent of semiconductor electronics and digital computers in the 1960s there have been dramatic advances in seismograph design, signal processing and seismic interpretation techniques. In this study we have made use of these advances to derive a substantially more detailed crustal model from new data.

GEOLOGY

Tectonic history and stratigraphy

The Kaapvaal Craton is one of the ancient nuclei around which the African continent is built (Fig. 1). The crystalline rocks constituting the bulk of the Craton are generally referred to as 'basement granites', although the term encompasses a range of compositions. The greatest ages obtained for the basement granites are about 3.55 Ga, with the intrusion of granitoids continuing sporadically until about 2.6 Ga (Tankard *et al.* 1982). Within the crystalline rocks are inliers of intensely metamorphosed and structurally deformed rocks known as greenstones, which are derived from sedimentary and volcanic strata. The suite of Archaean rocks constituting the Craton is known informally as the Basement Complex, of which the greenstone belts comprise less than 10 per cent of the exposure. A profound unconformity separates the Basement Complex from the relatively undisturbed supracrustal rocks, which cover most of the Craton except for a few isolated inliers such as the Johannesburg, Vredefort and Ventersdorp Domes (Fig. 2) and a 200 km broad strip along the northeastern margin of the Craton. Since 3.0 Ga the Kaapvaal Craton has been relatively stable, with tectonic movement providing the depositional environment for a succession of Archaean and Proterozoic basins exhibiting fluvial, deltaic and continental-shelf types of deposition. To the southwest, south and southeast the Craton is rimmed by the Proterozoic (2.1–0.9 Ga) Kalahari, Rehoboth and Namaqua Provinces (Fig. 1), which are thought to represent multiple amalgamation-accretion events (Hartnady, Joubert & Stowe 1985). These, in turn, are surrounded by the Pan-African (670–530 Ma) Damara and Saldania Provinces.

This study is confined to the central part of the Craton, largely within the limits of the Witwatersrand Basin. The rocks of the Dominion Group and Witwatersrand Supergroup are believed to have been deposited in the Witwatersrand Basin between 3.0 and 2.7 Ga (Walraven, Armstrong & Kruger 1990). The predominantly volcanic Dominion Group is known to reach a thickness of almost 3 km in the vicinity of the Klerksdorp goldfield (Tankard *et al.* 1982). The Witwatersrand Supergroup is divided into the predominantly argillaceous West Rand Group and a

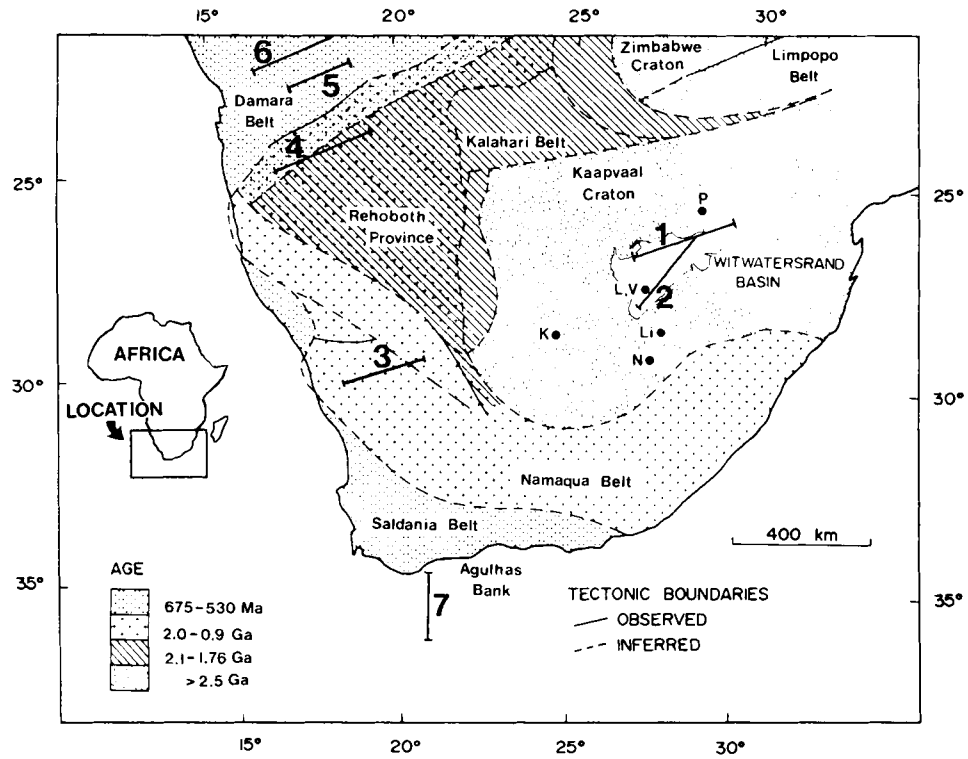

Figure 1. The major tectonic provinces of southern Africa (after Hartnady, Joubert & Stowe 1985), locations of kimberlites and deep seismic sounding experiments referred to in the text. Kimberlites: P—Premier, K—Kimberley, L—Lace, V—Voorspoed, N—Ngopetsoeu, Li—Lipelaneng. Deep seismic sounding experiments: 1, 2—Kaapvaal Craton (this study); 3—Namaqua Belt (Green & Durrheim 1990); 4-Rehoboth Province (Baier *et al.* 1983); 5, 6—Damara Belt (Baier *et al.* 1983); 7—Agulhas Bank (Hales & Nation 1972).

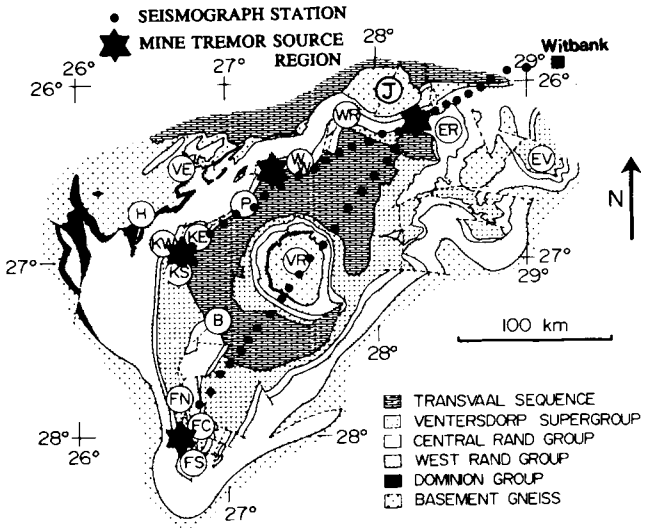

Figure 2. Geological map of the Witwatersrand basin with the Palaeozoic cover removed (after Borchers 1964; Jones 1988). Seismograph locations are indicated by dots. Granite domes are: J—Johannesburg, H—Hartebeesfontein, VE—Ventersdorp, and VR—Vredefort. Approximate localities of goldfields and gaps between them are: EV—Evander, ER—East Rand, WR—West Rand, WW—Far West Rand, P—Potchefstroom gap, KE—Klerksdorp east, KW—Klerksdorp west, KS—Klerksdorp south, B—Bothaville gap, FN—Free State north, FC—Free State central, and FS—Free State south.

predominantly arenaceous Central Rand Group, and reaches a thickness of almost 10 km in the centre of the basin. The Witwatersrand Supergroup is covered unconformably by the predominantly volcanic Ventersdorp Supergroup and the Transvaal Sequence consisting of dolomitic rocks, shale, lava and quartzite. Finally, Phanerozoic Karoo sediments, generally less than 400 m in thickness, cover much of the Witwatersrand Basin.

Vredefort structure

The Vredefort Dome, situated in the centre of the Witwatersrand Basin, is one of the Earth's largest cryptoexplosion structures. The dome of basement granite is about 40 km in diameter, and is surrounded by a collar of steeply dipping and overturned supracrustal strata (Nicolaysen 1990). Strong geochemical gradients within the granitic core are interpreted to indicate that the Archaean crust was turned 'on edge' during the updoming event. The Vredefort upper crust consists of massive granites or granite-gneisses, known as the Outer granite-gneiss (OGG). In the centre of the structure (10–15 km below the original cratonic surface) rocks of granitic composition, in granulite facies, predominate. This zone is termed the Inlandsee leucogranulite (ILG). In the centre of the structure a serpentinized ultramafic body has been intersected by a drillhole, and is interpreted to be a sample of mantle rock (Hart *et al.* 1990).

Kimberlites and xenoliths

The Kaapvaal Craton is the region of most concentrated kimberlite intrusion in the world. The kimberlites have transported numerous xenoliths from the mantle and lower crust to the surface. Over 90 per cent of all mantle xenoliths recovered in southern Africa belong to the peridotite suite and are composed of olivine with lesser orthopyroxene and minor garnet and/or clinopyroxene (Nixon 1987). They are thus garnet (spinel) lherzolites and harzburgites. Other mantle xenoliths include eclogites, pyroxenites, dunites and metasomites. Large numbers of mafic to felsic garnet granulites, interpreted as lower crustal xenoliths, have been recovered from kimberlites in the Namaqua Province (Dawson 1980). The handful of lower crustal xenoliths that have been recovered from kimberlites on the Craton originate from the Kimberley, Lace, Voorspoed, Ngopetseu and Lipelaneng pipes (Fig. 1). The specimens from the Craton are generally of granulite facies, and show a wide range of mineralogy (Carswell, Griffin & Kresten 1984; Van Calsteren *et al.* 1986; Dawson & Smith 1987; Harris *et al.* 1987). There are several possible explanations for the scarcity of lower crustal xenoliths recovered from kimberlites on the Craton: the lower crust was sparsely sampled by the kimberlites; fragments of the lower crust have been altered or assimilated; or the lower crustal xenoliths are so undistinguished in appearance that they have been overlooked by petrologists (Nixon 1987). It is probable that the mineralogy of the lower crust of the Kaapvaal Craton differs significantly from the adjacent Namaqua Province, lacking a significant component of garnets.

MINE TREMORS—THE SEISMIC ENERGY SOURCE

Explosives are generally used as the source of seismic energy in deep seismic sounding experiments, but in this study we made use of mine tremors induced by deep-level mining in the major goldfields of the Witwatersrand basin. The violent failure of stressed rock in the vicinity of mining operations is a major hazard of deep-level gold mining. Mining-induced seismic events range in local magnitude (M) from −6 to +5 on the Richter scale. The majority of seismic events have their focus within tens of metres of advancing longwall mining faces (Cook 1963), which are typically located at depths of 1–4 km. It has been established that the level of mine tremor activity is related to the volume of rock removed and the depth of mining (McGarr 1976). However, further differences in the level of seismicity exist between the various goldfields, which are attributed to local geological structure. Most of the larger events are associated with geological discontinuities such as faults and dykes (Arnott 1981; Potgieter & Roering 1984; Gay *et al.* 1984).

Studies of mine tremors have shown that they are very similar to natural crustal earthquakes with regard to stress drops, the relationship between moment and magnitude, and the relationship between rock failure dimension and magnitude. The parameters of the mine tremor source can be estimated from the corner frequency using the model of Brune (1970, 1971). In a study of 24 mine tremors from the East Rand goldfield with magnitudes in the range $M = 0$–3, the calculated source radius ranged from 50 to 500 m and the ratio of P- and S-wave energy was found to have a median of 0.18 with a range of 0.005 to 1.1 (Spottiswoode & McGarr 1975). The radiation pattern for a tremor is more complicated than that for an explosive source. An explosive seismic source produces dominantly compressive waves with

a radiation pattern that is concentric about the source. In contrast, the seismic energy radiation pattern produced by an earthquake double-couple source mechanism produces both compressional and shear energy. The nodal planes of the *S*-wave radiation pattern are rotated by 45° with respect to the nodal plane of the *P*-wave pattern. This implies that the maximum compressive displacement coincides with the minimum shear displacement, and vice versa (Kasahara 1981). In practice, however, the radiation pattern is not generally uniform for the entire rupture process, and so the actual occurrence of nodal planes is considered unlikely. The variation of amplitude with distance from the epicentre is not just a function of the ray path and the site effect, but also of the orientation of the fault plane and the direction of slip of the particular tremor.

During the course of the deep seismic sounding experiment it was found that events with $M > 3$ were required to produce a satisfactory signal to noise ratio at distances exceeding 200 km. The cumulative distribution of magnitudes for various South African gold mining districts during a three and a half year period which includes the duration of the experiment, and the year preceding it, is shown in Fig. 3. It is apparent that the Far West Rand goldfield is the most seismically active district, producing about 10 events with $M > 3$ per month. The Klerksdorp goldfield releases almost as much seismic energy, but tends to have more large events. The East Rand and Orange Free State (OFS) goldfields have relatively low levels of seismic activity, producing on average only about two events with $M > 3$ per month.

The South African Seismological Network (SASN) consists of 23 stations distributed throughout South Africa. The location, origin time and magnitude of events which produce good-quality *P*-wave arrivals on at least four stations are published in the monthly Seismological Bulletin of the South African Geological Survey. Most mine tremors with $M > 2$ fulfil this criterion. The arrival times of the *P*- and *S*-waves are read from the SASN seismograms with an accuracy of 0.1 s at best. Consequently the standard deviations in the location, origin times and magnitude are quite large, typically of the order of ±5 km, ±0.5 s and ±0.15 respectively. During the experiment a single tremor

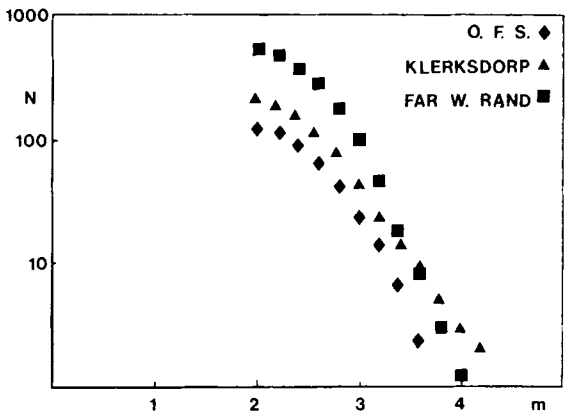

Figure 3. Magnitude–frequency distribution for mine tremors in the Witwatersrand goldfields for the period January 1985 to May 1988 (after Fernandez *et al* 1988). N = cumulative number of events of magnitude m per year.

was usually recorded at several stations along the profile, so the phase velocities between the stations could be accurately determined. Further, several events from a particular goldfield were recorded at each station. This multiplicity of events allowed 'static shifts' to be made to the seismograms to account for errors in source location and origin time. The residual errors in the record sections are difficult to quantify, but we estimate that the maximum error in the shot–receiver distance is 3 km, and in the traveltime is 0.2 s. The average errors are estimated to be about 1 km and 0.1 s respectively.

The use of tremors for deep seismic sounding has several advantages: it is relatively cheap as no shot holes have to be drilled or explosives expended; stations may be occupied until an adequate number of tremors are recorded; the large amount of shear energy produced in addition to compressive energy allows the *P*- and *S*-waves to be jointly analysed; and the tremors have wide bandwidth, producing substantial energy at frequencies as low as 1 Hz. Unfortunately several difficulties also arise from the use of tremors: the source location and origin time are imperfectly known; the source region may be several hundred metres in dimension; the position of the source is limited to the mining areas; seismograms from tremors with a range of magnitudes and source mechanisms are used to compile a record section, making phase correlation more difficult; and the experiment takes a longer period to complete.

SEISMIC EXPERIMENT

Data acquisition

Seismographs were deployed at approximately 10 km intervals along two profiles (Fig. 2). Observations were made between March 1986 and July 1988. The maximum number of stations that could be simultaneously maintained was six. Three-component sets of critically damped 1 Hz ELECTROTECH EV17 and EV17H seismometers were used. The time-reference for the portable multichannel seismograph (Green 1973) is provided by both a radio and internal clock. As reception of the radio signal is erratic, a portable master clock was used to provide an additional absolute time reference. Station locations were plotted on 1:50 000 scale topographic maps. The accuracy of the station coordinates and elevations are estimated to be better than 100 and 10 m respectively.

Data processing

The field tapes were replayed with an anti-alias filter and digitized. As the record speed of the tape decks varied somewhat, the sampling rate ranged from 60 to 100 Hz, but was usually about 80 Hz. The sampling rate and lead or lag of the internal clock for each recording period were determined by examining the digitized master and seismograph clock signals. The accuracy of timing is estimated to be about twice the sampling interval i.e. about 25 ms for a seismogram digitized at 80 Hz. This is far smaller than errors introduced by uncertainties in the origin time and location of the mine tremors. Standard Fourier frequency domain band-pass filters were used to reduce noise. The seismograms displayed in the record sections

have all been filtered using a passband that rises from zero at 0.5 Hz to unity at 2 Hz, remains at unity to 8 Hz, and decreases to zero again at 12 Hz. The flanks of the frequency domain filter have the shape of a cosine function (between 0 and π).

Data display

Vertical component seismograms with good signal-to-noise ratios and showing clear definition of the various phases were selected for display. In a few instances the vertical component failed, and a horizontal component which shows phases that can be clearly correlated with the vertical component seismograms recorded at adjacent stations is plotted. For clarity of display seismograms were selected at regular offset increments for plotting. Record sections are presented at two time-scales: a 12 s window showing the *P*-wave arrivals using a reduction velocity of 6 km s^{-1}, with arrivals having velocities less than 4 km s^{-1} muted as the large-amplitude *S*- and surface waves tend to dominate the trace; and a 24 s window showing the *S*-wave arrivals using a reduction velocity of 3.464 km s^{-1}. The seismograms are normalized to the maximum amplitude on each trace. The *S*-wave record section was plotted with a reduction velocity of 3.464 km s^{-1} ($6/\sqrt{3}$) and the time axis compressed by a factor of $\sqrt{3}$ relative to the *P*-wave section in order to facilitate comparison with the *P*-wave record section. If Poisson's ratio is 0.25 throughout the crust and upper mantle, this scaling causes the *P*- and *S*-wave traveltime curves to match precisely. Any deviation indicates variations in Poisson's ratio from 0.25 (Holbrook *et al.* 1988). The record sections are shown in Figs 4–8. Hand-drawn traveltime curves are superimposed on the record sections, with the phase correlations and apparent velocity (in km s^{-1}) indicated.

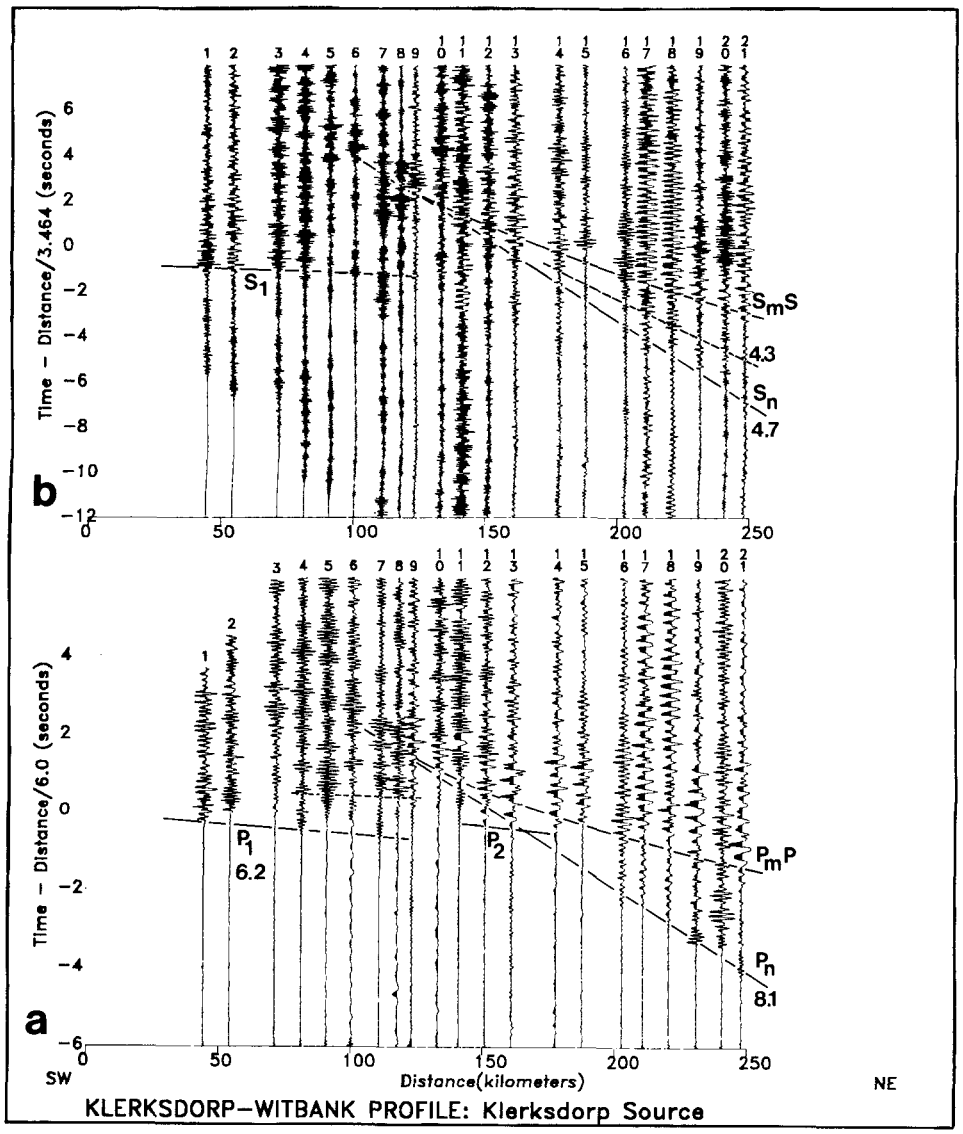

Figure 4. Record sections for the Klerksdorp–East Rand–Witbank profile. Tremors from the Klerksdorp goldfield.

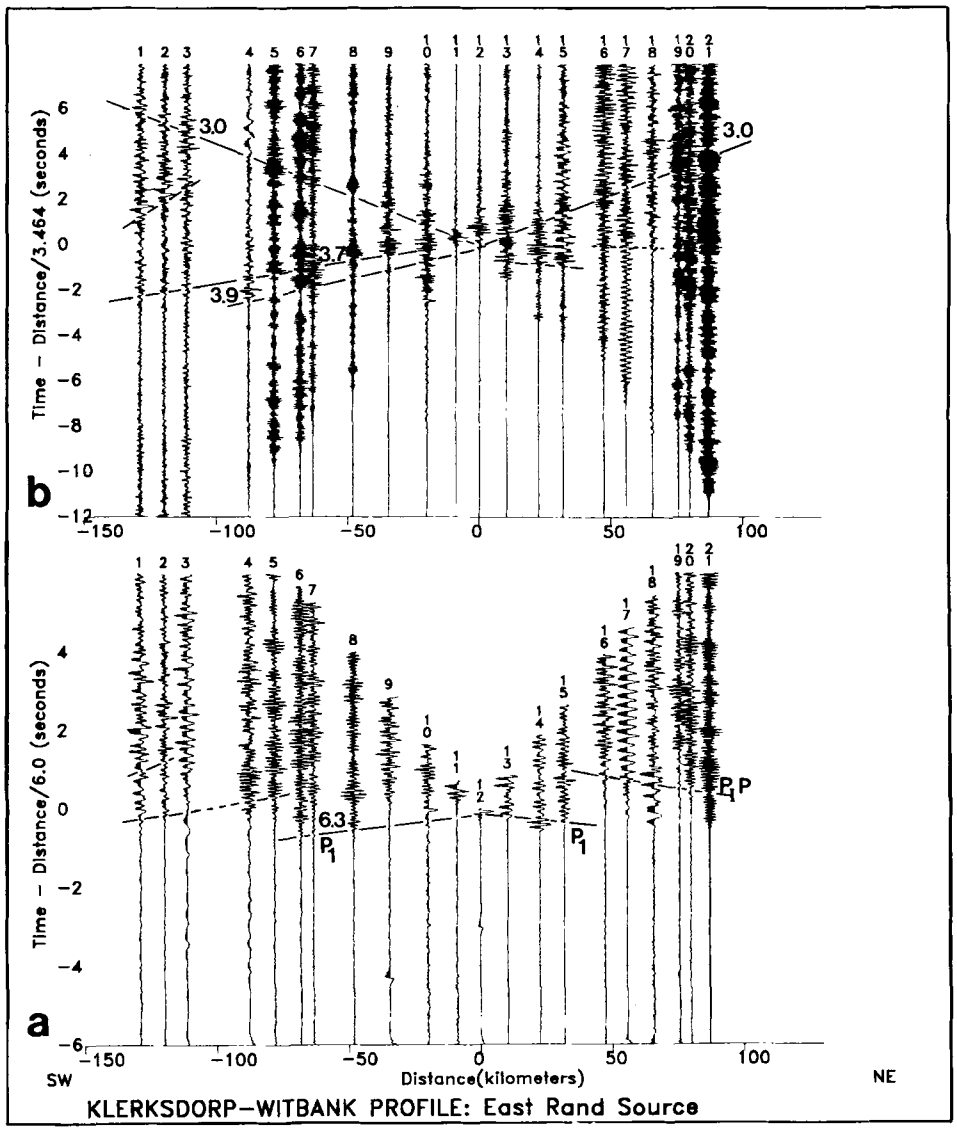

Figure 5. Record sections for the Klerksdorp–East Rand–Witbank profile. Tremors from the East Rand goldfield.

INTERPRETATION

Method

Once the record sections had been compiled the analysis generally followed the scheme outlined below.

(a) Correlation of the phases in the record section.

(b) Identification of phases as refracted or reflected arrivals. The following symbols have been used to denote the various phases:

P_1, S_1—direct wave travelling in the upper crust;

P_1P, S_1S—reflection from a mid-crustal discontinuity;

P_n, S_n—refracted wave arising at the Moho;

P_mP, S_mS—reflection from the crust/mantle transition.

(c) Interpretation of first arrivals using slope-intercept methods.

(d) 1-D interpretation of first and secondary P-wave arrivals using the Herglotz–Wiechert approach and methods described by Slichter (1932) and Giese (1976). The album of synthetic record sections calculated for a range of velocity transitions (Braile & Smith 1975) also proved useful in developing a velocity model.

(e) Ray tracing was used to compute synthetic record sections for 1-D and 2-D models. The program RAYAMP-PC, written by D. Crossley of the Geophysics Laboratory, McGill University was used. It is an interactive microcomputer version of the program RAYAMP (Spence, Whittall & Clowes 1984). The velocity structure is represented by large polygonal blocks, within which the velocity gradient is uniform and of arbitrary orientation. Amplitudes of reflected and refracted waves are determined using zero-order asymptotic ray theory, and the amplitudes of head waves by means of first-order asymptotic ray theory. The fit between the synthetic and observed data was improved by adjusting the model, using geological information as constraints. The seismic velocity, density and thickness of the major geologic units constituting the Kaapvaal Craton are listed in Table 1.

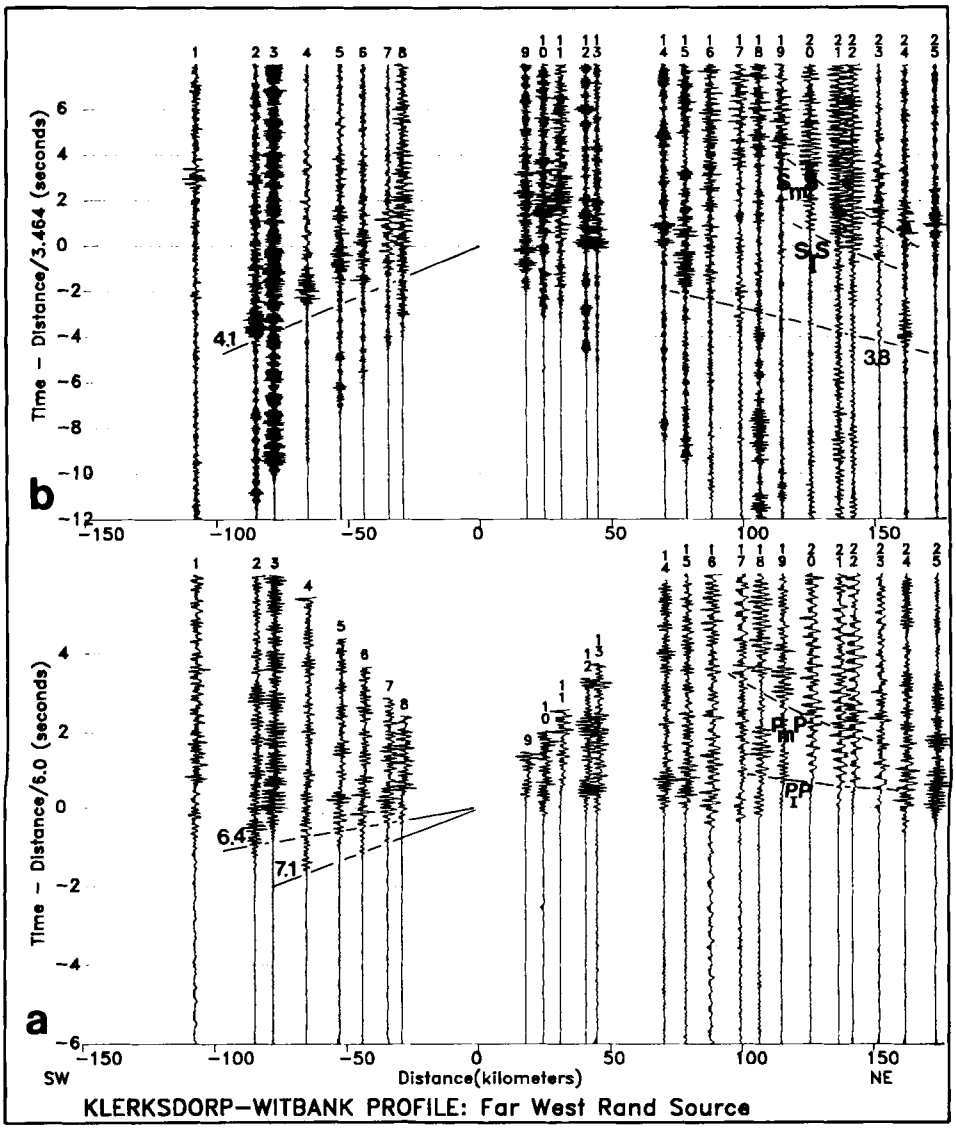

Figure 6. Record sections for the Klerksdorp–East Rand–Witbank profile. Tremors from the Far West Rand goldfield.

(*f*) The 2-D interpretation of *S*-wave arrivals was carried out by initially using the geometry of the *P*-wave model and assuming a Poisson's ratio of 0.25. In order to improve the fit between observed and calculated arrivals the *S* velocities were first varied. The positions of the interfaces were only adjusted as a last resort.

(g) The reflectivity method (Fuchs & Müller 1971) was used to compute synthetic seismograms for a generalized 1-D model of the Kaapvaal Craton in order to evaluate the effect of attenuation and velocity gradients in the mid-crust, crust–mantle transition and upper mantle on the amplitude and frequency of the arrivals.

Error estimates in refraction modelling are difficult to make because quantifiable uncertainties (e.g. from scatter in traveltime data and misfits between calculated and observed traveltimes) are usually much smaller than the uncertainties introduced by the interpretative step of phase correlation (Holbrook *et al.* 1988). This uncertainty is well illustrated by the range of interpretations produced by workers analysing the same data set (the 1978 Saudi Arabian refraction profile), but making different phase correlations (Mooney & Prodehl 1984). Major features such as the depth to Moho and velocities in the upper crust and upper mantle are reliably determined. More subtle intracrustal features, such as low-velocity layers and velocity gradients, give rise to a greater variation in interpretation. In the models produced in this study we consider the determination of the velocities and the depths of the interfaces to be better than 0.2 km s^{-1} and 2 km respectively. Greater changes in the model noticeably degrade the fit of the synthetic record section to the observed data.

Qualitative interpretation of record sections

In the following discussion it is often necessary to refer to a particular wave group on the record sections. The trace number and reduced traveltime are used to specify the feature.

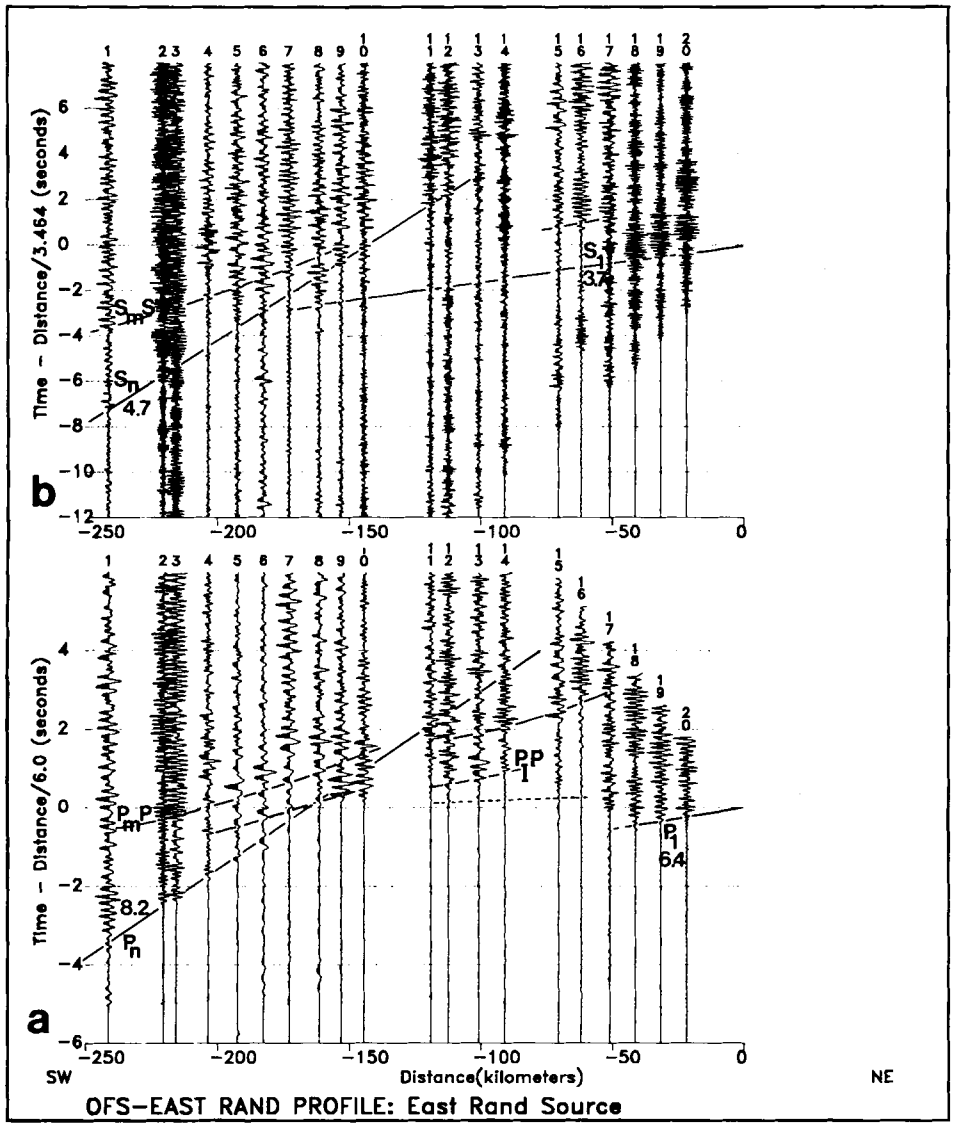

Figure 7. Record sections for the OFS–East Rand–Witbank profile. Tremors from the East Rand goldfield.

Surface waves. Surface waves are generally not prominent on the record sections. Shapira (1988) notes that South African mine tremors show well-developed R_g-waves with the fundamental mode propagating at 3.1 km s^{-1} and a dominant frequency of about 1 Hz on seismograms recorded by the South African Seismological Network (SASN). The SASN seismographs have a bandwidth of 0.5–2.5 Hz, while the record sections shown here have been digitally filtered with a passband of 2–8 Hz. The seismograms are dominated by energy at frequencies greater than 5 Hz, which has generally obscured the low-frequency surface waves.

Extinction of the first arrival. The first arrival phase (P_1) is impulsive as far as offsets of 30–50 km. Thereafter it has an emergent character. This phase is extinguished at offsets of 50–140 km, depending on the profile. The Central Rand Group, in which the focus of most tremors is situated, has a considerably lower velocity than the overlying Ventersdorp Supergroup lavas (5.7–6.0 km s^{-1} and 6.4 km s^{-1} respectively). Upgoing waves striking this interface with an angle of incidence greater than 70° will be totally reflected. The focus of most tremors is within 2 km of this interface. This implies that only rays striking the interface within a radius of about 6 km of the epicentre are transmitted directly to the layer above. As the overlying layer (the Ventersdorp lavas) has a greater velocity, the transmitted rays are refracted away from the normal. Consequently the amplitude of the transmitted wave will decline with offset. Energy may also be transmitted to large offsets by reverberations within the supracrustal strata.

Upper/lower crust transition. A wave group with a high amplitude, low dominant frequency and early reduced traveltime is recorded as a first arrival at distances of 150–180 km on the Klerksdorp–Witbank record section (see phase labelled P_2 on traces 12 and 13 in Fig. 4a). The features of this phase are best explained by a mid-crustal velocity gradient. The record sections to the northeast and southwest of the East Rand goldfield (Figs 5 and 7), as well as northeast of the Far West Rand goldfield (Fig. 6) display

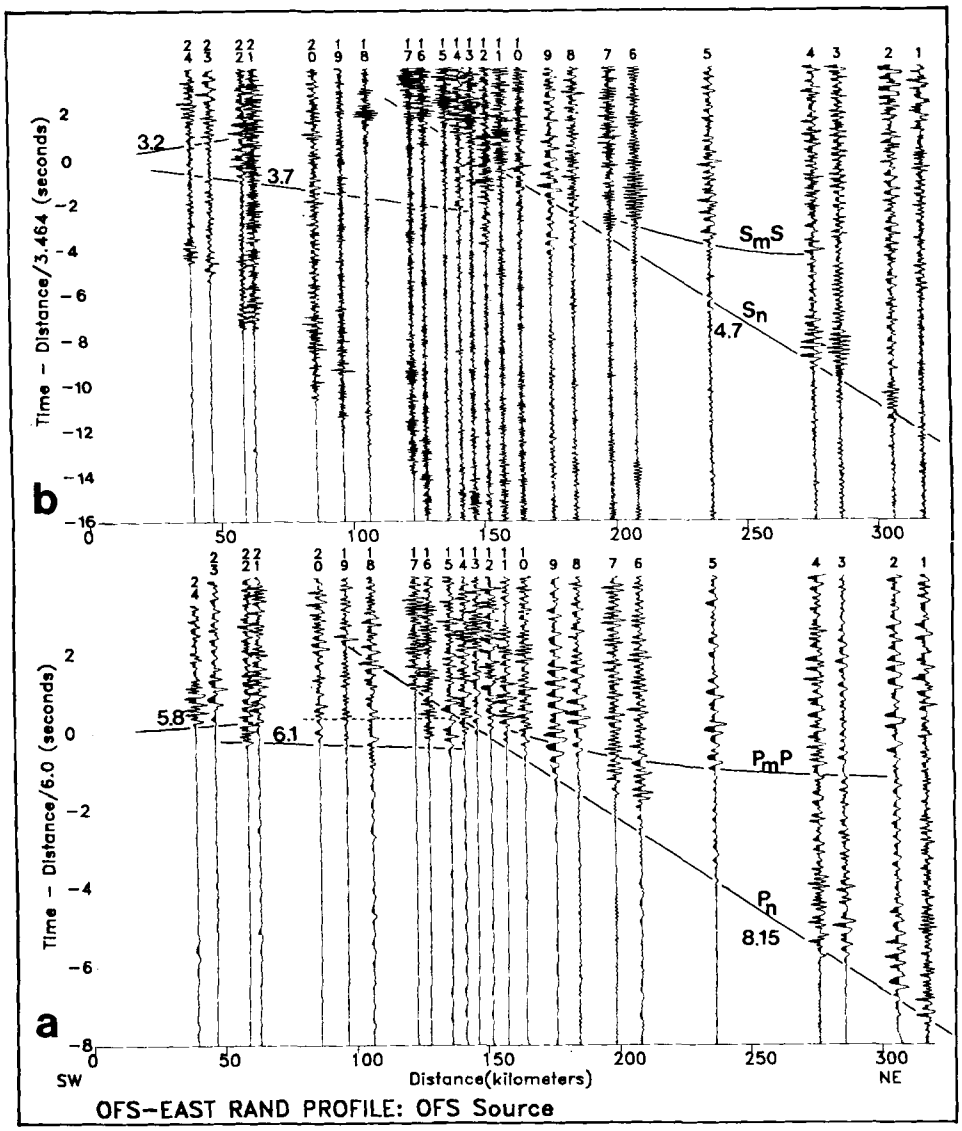

Figure 8. Record sections for the OFS–East Rand–Witbank profile. Tremors from the OFS goldfield.

a clear second arrival phase (labelled P_1P), substantially retarded with respect to the first arrival, which appears at offsets greater than 50 km. This phase is most simply interpreted in terms of a mid-crustal velocity discontinuity. $T^2 - X^2$ analysis indicates that the reflector is at a depth of about 16 km. A substantial velocity contrast (e.g. 6.2 to 6.6 km s^{-1}) is required to produce a supercritical reflection at a distance of about 60 km.

Crust/mantle transition. If the Moho were a first-order discontinuity the S_mP and P_mS phases would constructively interfere, and produce amplitudes as large as the supercritical P_mP phase. However, a transition zone with a linear velocity gradient and thickness equal to the dominant wavelength of the P-wave, reduces the amplitude of the converted phase reflection to 10 per cent of that produced by a first-order discontinuity (Fuchs 1975). Although, on average, 80 per cent of the energy radiated by a tremor is shear energy, the S_mP phase has not been identified on the record sections. This suggests that the crust/mantle boundary is not a sharp discontinuity, but a transition zone several kilometres in thickness.

Attenuation of the P_mP *and* S_mS *phases.* The P_mP is observed to have a low dominant frequency relative to the P_n phase, and a long duration. This is observed on all the record sections, but most prominently on the Klerksdorp–Witbank profile (traces 17–21, Fig. 4a). At offsets greater than 200 km more than half the travelpath of the P_n phase is in the upper mantle, while the entire travel path of the P_mP is in the crust and crust/mantle transition zone. We believe that the relatively greater attenuation and dispersion of the P_mP phase occurs in the crust and crust/mantle transition zone.

Attenuation may be intrinsic, where seismic energy is absorbed by anelastic processes in the rock such as frictional dissipation due to relative motions at grain boundaries and across crack surfaces, flow and 'squirting' in fluid-filled pores, and relaxation due to shear motions at pore–fluid

Table 1. Representative seismic velocity, density and maximum thickness of formations constituting the Kaapvaal Craton. Source of data: (a) Roux (1970), (b) Campbell & Peace (1984), (c) Green & Chetty (1990), (d) Stepto (1979), (e) Pretorius, Jamison & Irons (1989), (f) Weder (1990). The maximum thicknesses are rough estimates gleaned from a variety of sources.

	maximum thickness (km)	density (g/cm^3)	P-wave velocity (km/s)
KAROO SEQUENCE			
sandstone & shale	1	2.65[b]	3.5[b]
TRANSVAAL SEQUENCE			
Pretoria Group			
shale, lava & ferruginous			
quartzite	4	2.85[a]	5.5-6.3[c]
Chuniespoort Group			
dolomite	2	2.88[b]	6.8[b]
VENTERSDORP SUPERGROUP			
lava	4	2.85[b]	6.4[b]
WITWATERSRAND SUPERGROUP			
Central Rand Group			
quartzite	3	2.65[b]	5.7[b]
West Rand Group			
ferruginous shale &			
quartzite	7	2.80[a]	5.7-6.1[b,e,f]
DOMINION GROUP			
lava	3	not available	
BASEMENT COMPLEX			
Outer granite-gneiss		2.65[d]	6.0[c]
Inlandsee leucogranulite		2.84[d]	6.4[c]

boundaries (Toksöz & Johnston 1981). Scattering of seismic energy by heterogeneities within the crust (Richards & Menke 1983) and the generation of multiples by small-scale crustal layering (Schoenberger & Levin 1974) also gives rise to 'apparent' attenuation. At source–receiver distances greater than twice the target depth, waves scattered from a random zone have the same appearance as waves reflected from a laminated zone, and these two mechanisms cannot easily be distinguished (Gibson & Levander 1988). The attenuation effects due to absorption and scattering are approximately additive. Several diagnostics have been proposed to determine the dominant mechanism, the most applicable in this case being the measurement of the frequency content of the wave coda. The coda of the wave which has been scattered will contain higher frequencies than the initial pulse, while the coda of a wave that has experienced absorption will not (Richards & Menke 1983). Inspection of the frequency spectra of traces 17–21 (Fig. 4a) does not reveal any systematic increase of frequency within the P_mP-wave group. This would suggest attenuation due to absorption. In contrast, the S_mS-wave group does show a marked increase in frequency with time (see especially traces 19–20, Fig. 4b). This could indicate scatterers in the crust. To roughly estimate the scalelength of the S-wave scatters we use the result of Raynaud (1988) that scattering is peaked at the frequency for which the seismic wavelength is approximately six times greater than the scalelength of the elastic variations. The backscattering model of Wu & Aki (1985) yields a similar result. Thus for an S-wave with a velocity of 3.6 km s^{-1} and frequency of scattering of 10 Hz, the correlation length of the scatterers is about 60 m. The absence of P-wave scattering may be due to the inherently longer wavelength of the P-wave.

Most field measurements of attenuation in the continental crust have used surface waves to obtain estimates of S-wave attenuation (Q_S). Relatively few measurements of P-wave attenuation (Q_P) have been made. Attenuation coefficients obtained for stable regions of North America and Eurasia are nearly identical within the limits of observation: the upper 15–20 km of the crust yields values of Q_S in the range 250–1000, while greater depths have $Q_S > 1000$, and show little regional variation (Mitchell, Yacoub & Correig 1977). The exceptionally high values of Q obtained in the lower crust have been attributed to the absence of water—laboratory measurements show an increase in the Q of low-porosity olivine basalt from 100 to 2000 when outgassed (Tittman 1977). Consequently, should the lower crust contain a significant amount of fluid in pores, a low value of Q would be expected. In this context it is significant that the unusually low electrical resistivity observed at the base of the crust of the Kaapvaal Craton has been attributed to the presence of hydrated minerals or saline pore water at high fluid pressures (Van Zijl 1978; Percival & Berry 1987). A study of the attenuation of high-frequency (3–30 Hz) S- and L_g-waves in the Kaapvaal Craton found the value of the L_g-wave Q to be 360 at 3 Hz (Frankel *et al.* 1990). This is considered to be surprisingly low for a tectonically stable area, and it is suggested that structural complexities along the path, low-velocity zones within the crust, and interfaces above the seismic source may all contribute to the unusual attenuation.

We conclude that there are possibly several mechanisms which contribute to the attenuation of the P_mP and S_mS phases: anelastic absorption in the lower crust (due to the presence of water-filled pores or hydrated mantle rock), scattering due to heterogeneties with a spatial dimension less than 100 m, and reflection from a zone of finely layered structure in the lower crust.

Sub-Moho velocity structure. The P_n phase is observed to have very small amplitudes between 170 and 200 km, while strong P_n and S_n phases are observed beyond 200 km. This may be explained by the existence of a velocity gradient below the Moho. A positive sub-Moho velocity gradient produces refracted waves with an amplitude minimum at some distance after the critical point, followed by a maximum, and then decreasing again (Červený, Molotkov & Pšenčík 1977). The precise position of the minimum and maximum depends on the details of the velocity model.

Ray-trace modelling

The objective of 2-D ray-tracing modelling is to reproduce the major features of the observed record sections with a plausible earth model. The synthetic seismograms are normalized by the maximum amplitude on each trace (the same scaling method was applied to the observed record sections). The geometric symbols on the synthetic record sections indicate some of the observed traveltimes that were used to constrain the modelling. Selected rays are

superimposed on the velocity model to show the travelpath of each phase. At each interface the velocity (km s^{-1}), and velocity gradient (s^{-1}) except where it is less than 0.01 s^{-1}, are indicated.

In some cases we experienced difficulty in reproducing the *S*-wave observations with a model having the same geometry as that derived for the *P*-wave data, even if alternative phase correlations were considered. The *S*-wave phases are found to be quite variable, especially when all three components from several tremors are considered. This probably due to variations in the focal mechanisms and radiation patterns of the tremors. The *S*-wave models we present here represent our best attempt to interpret the data objectively.

Klerksdorp–Witbank profile

The 2-D *P*- and *S*-wave models, ray traces and synthetic record sections for mine tremors in the Klerksdorp goldfield are shown in Fig. 9. The seismic source is located at a depth

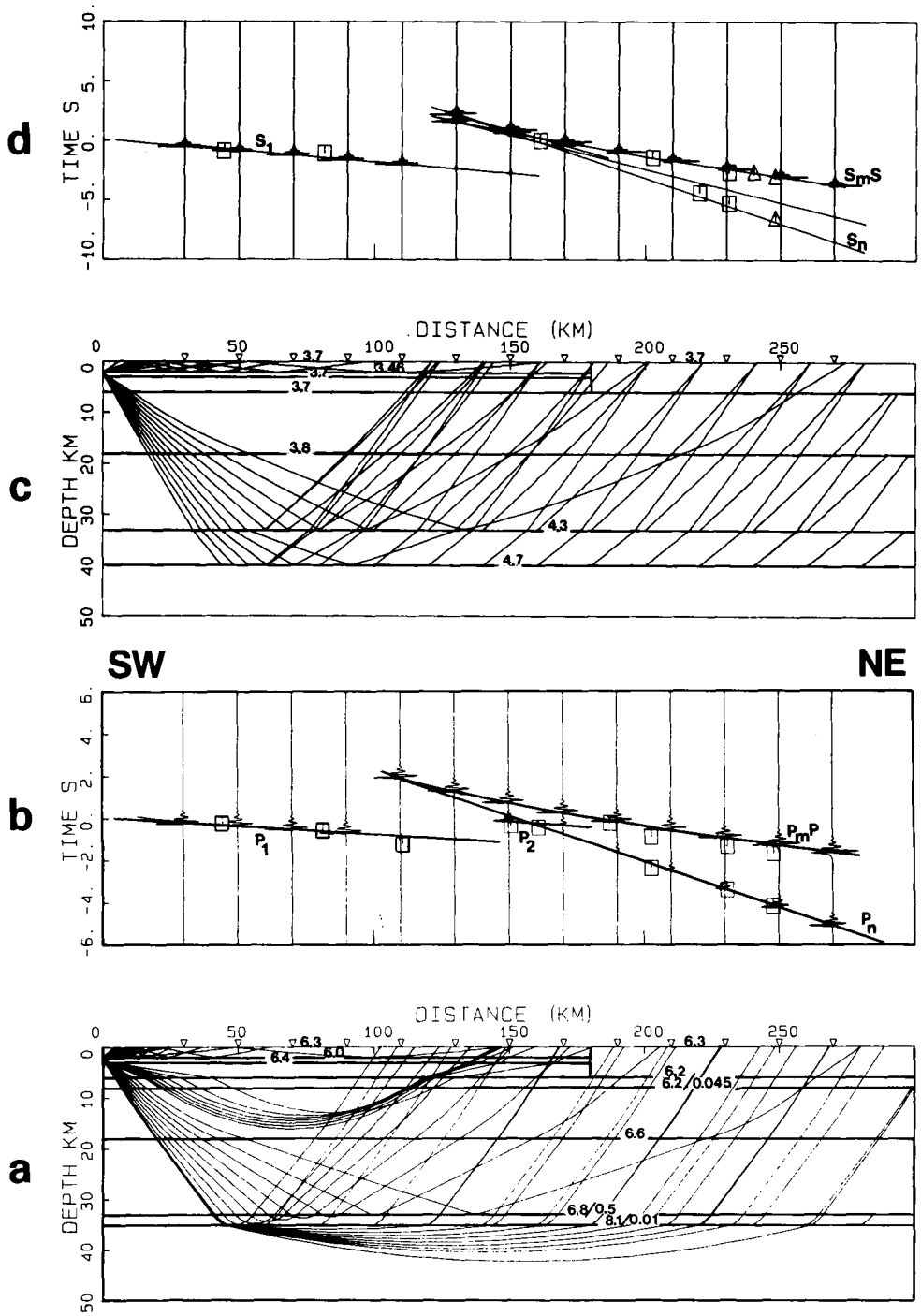

Figure 9. Velocity model, ray-trace diagram and synthetic record section for the Klerksdorp–East Rand–Witbank profile. Tremors from the Klerksdorp goldfield. Reduction velocities: (a) 6 km s^{-1}; (c) 3.464 km s^{-1}.

of 2.5 km, within a layer assigned a velocity of 6 km s^{-1}. This layer represents the quartzites of the Central Rand Group. The overlying Ventersdorp Supergroup and Transvaal Sequence strata have been assigned a uniform *P*-wave velocity of 6.3 km s^{-1}, and the underlying dense shales of the West Rand Group a velocity of 6.4 km s^{-1}. This is considerably higher than the maximum velocity for the West Rand Group cited in Table 1. The tabulated velocities were measured in boreholes which did not deeply penetrate the West Rand Group. Horizontal layers have been used to represent the supracrustal strata, although it is known that there is considerable faulting within the Witwatersrand basin. The wide (10 km) spacing of the seismographs as well as the considerable size of the goldfields from which the tremors originate (the Klerksdorp and Far West Rand goldfields each extend for about 25 km along the basin margin) make it impossible to resolve the structure of the supracrustal strata in this experiment.

Strong impulsive direct waves are only observed to an offset of about 50 km in the data. Beyond this the first arrivals become relatively weak and emergent in character (Fig. 4a). These observations are modelled by a strong increase in velocity in the layer above the source, causing much energy to be trapped within the low-velocity Central Rand Group layer (Fig. 9a). In the model, direct arrivals are only detected within 30 km of the source. At greater distances the energy propagates within the uppermost layer by multiple reflection, giving rise to weak first arrivals.

The high-amplitude wave group (P_2) observed at offsets of 150–180 km is considered to be produced by a velocity gradient within the crystalline basement. It is modelled by a 10 km thick gradient zone commencing at a depth of 8 km, with a gradient of 0.045 s^{-1}. The lower crust (18–33 km) is modelled by a layer with a uniform velocity of 6.6 km s^{-1}. The crust/mantle transition is modelled by a layer with a linear velocity gradient of 0.5 s^{-1} between 33 and 35 km. This zone produces diving waves and wide-angle reflections at distances beyond 100 km. The P_n phase is observed to have relatively large amplitudes at offsets greater than 200 km. In order to produce this feature, a layer 10 km thick and with a gradient of 0.01 s^{-1} is introduced below the Moho.

The *S*-wave model is shown in Fig. 9(c). The upper crystalline crust is assigned a velocity of 3.66 km s^{-1} at a depth of 6 km, increasing gradually (0.015 s^{-1}) with depth. No indication of a steep mid-crustal *S*-wave velocity gradient is observed. The most prominent wave group on the observed record section is the S_mS phase (Fig. 4b). For Moho at a depth of 35 km (the Moho depth of the *P*-wave model), an average crustal velocity of 3.8 km s^{-1} is required to match the observed traveltime curve, and the S_n phase is best replicated by an upper mantle velocity of 4.5 km s^{-1}. However, the observed S_n velocities are somewhat higher (4.7 km s^{-1}). A more satisfactory fit is achieved by shifting the position of the *S*-wave Moho to a depth of 39 km, and introducing a discontinuity at 33 km where the velocity increases to 4.3 km s^{-1}. This produces both the S_mS phase and the arrivals observed mid-way between the S_n and S_mS phases (see Fig. 4b). The rather weak amplitudes of the S_n phase are modelled by a slight sub-Moho velocity gradient.

The *P*-wave record section observed for tremors originating in the East Rand goldfield is modelled using a virtually identical model to that for Klerksdorp tremors—the only difference is a slightly greater velocity gradient in the upper crust (Fig. 10a). To the northeast of the source region the mid-crustal velocity gradient is replaced by a

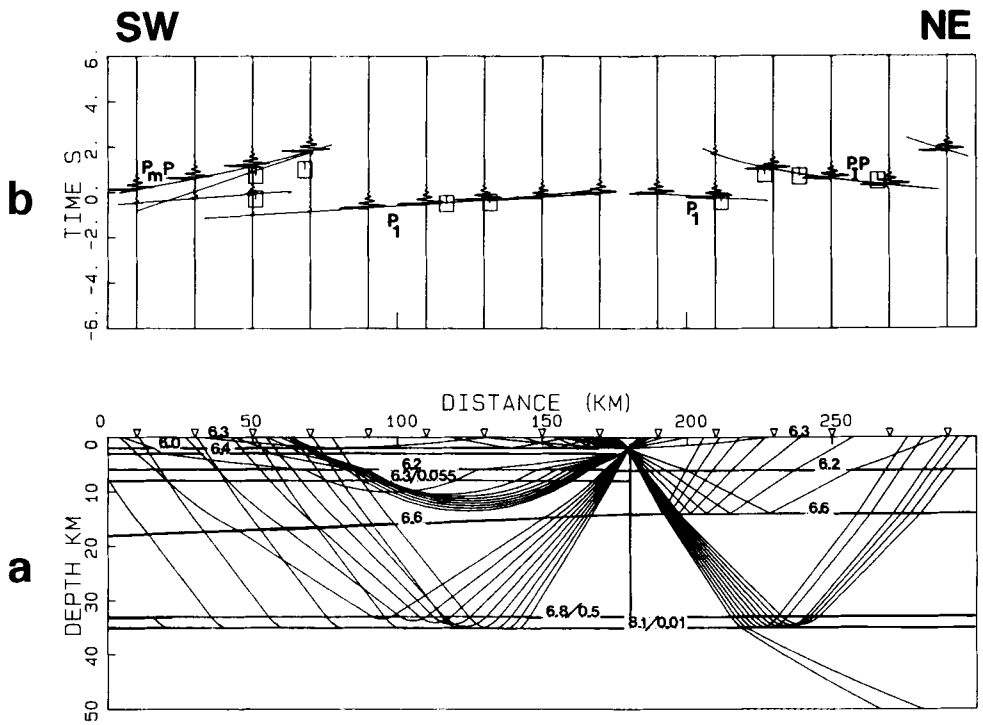

Figure 10. Velocity model, ray-trave diagram and synthetic record section for the Klerksdorp–East Rand–Witbank profile. Tremors from the East Rand goldfield. Reduction velocity 6 km s^{-1}.

velocity discontinuity at a depth of 14 km to produce the P_1P phase (Fig. 5a). A velocity contrast of about 0.6 km s^{-1} is required to produce critical reflections at an offset of 70 km. The main features of the *S*-wave record sections can be reproduced with a model having the same geometry as the *P*-wave model. The correlation and identification of the later *S*-wave phases are uncertain, and so it was not attempted to model the finer details of the *S*-wave record section.

The Klerksdorp–Witbank profile passes about 20 km to the south of the Far West Rand goldfield; consequently the seismic stations form a fan, and each ray path has a different azimuth. The record sections for tremors originating in the Far West Rand are shown in Fig. 6. The *P*-wave record section for tremors occurring in the Far West Rand goldfield (Fig. 6a) is similar to that for the East Rand source region (Fig. 5a). To the southwest of the source the very fast (6.8 km s^{-1}) first arrivals are produced by energy travelling

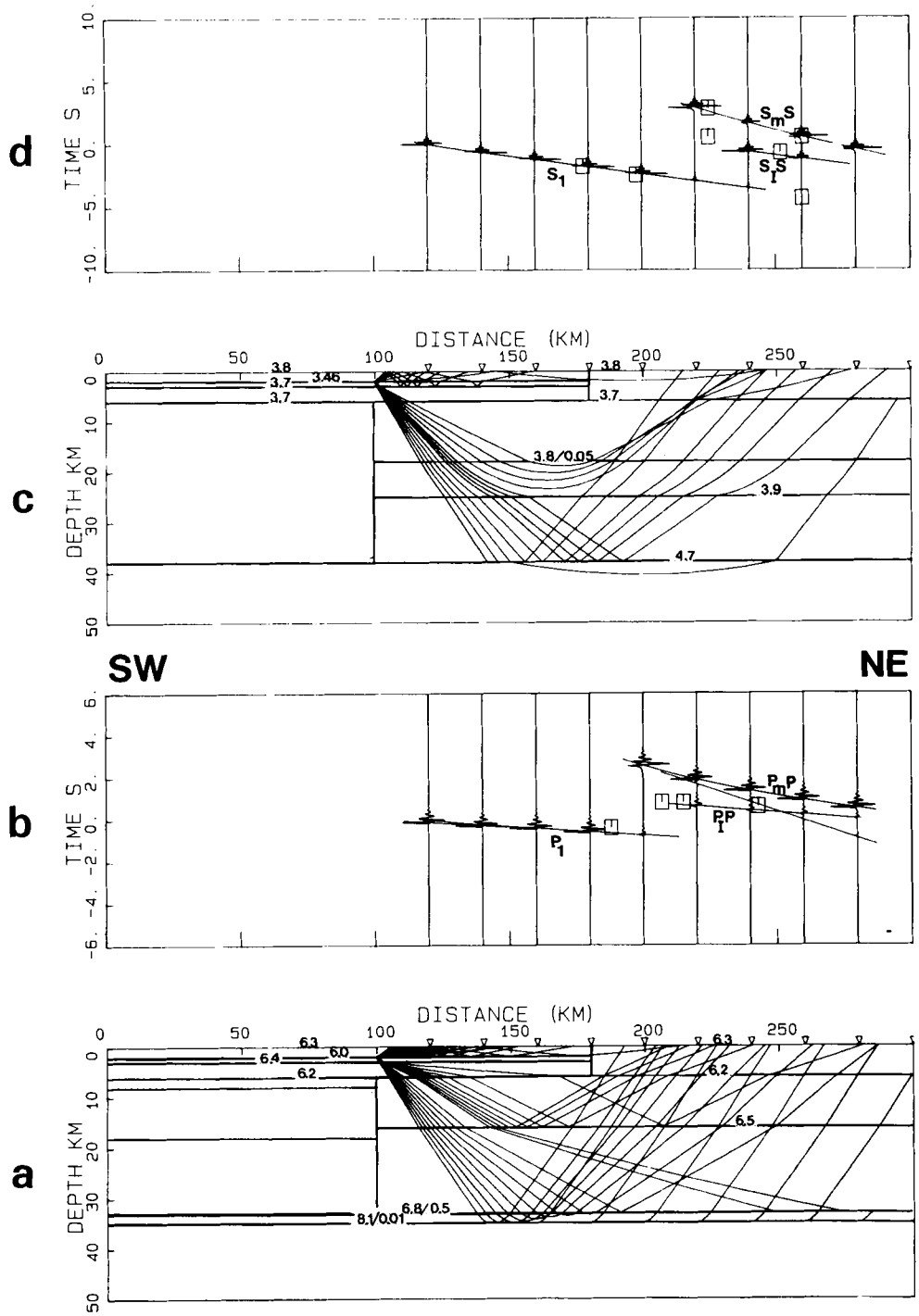

Figure 11. Velocity model, ray-trace diagram and synthetic record section for the Klerksdorp–East Rand–Witbank profile. Tremors from the Far West Rand goldfield. Reduction velocity: (a) 6 km s^{-1}; (c) 3.464 km s^{-1}.

within the high-velocity dolomitic rocks of the Transvaal Sequence. The second arrival which is observed beyond 100 km to the northeast is identified as a P_1P phase, and modelled by a mid-crustal velocity discontinuity at a depth of 16 km (Fig. 11a). The first *S*-wave arrival beyond 60 km has a high velocity (3.8 km s^{-1}) and is detected right to the end of the profile. The phase was satisfactorily modeled by reverberations within the supracrustal strata (Fig. 11c). The S_1S phase is characterized by high-amplitude arrivals at distances between 120 and 150 km (Fig. 6b). In order to model this phase, a velocity gradient of 0.05 s^{-1} was introduced between 18 and 25 km. The *S*-wave Moho is modelled at a depth of 38 km, but as this profile does not extend beyond the cross-over distance, this depth is not well constrained.

Orange Free State–East Rand profile

Tremors originating in the OFS goldfield were recorded while seismographs were deployed between the East Rand

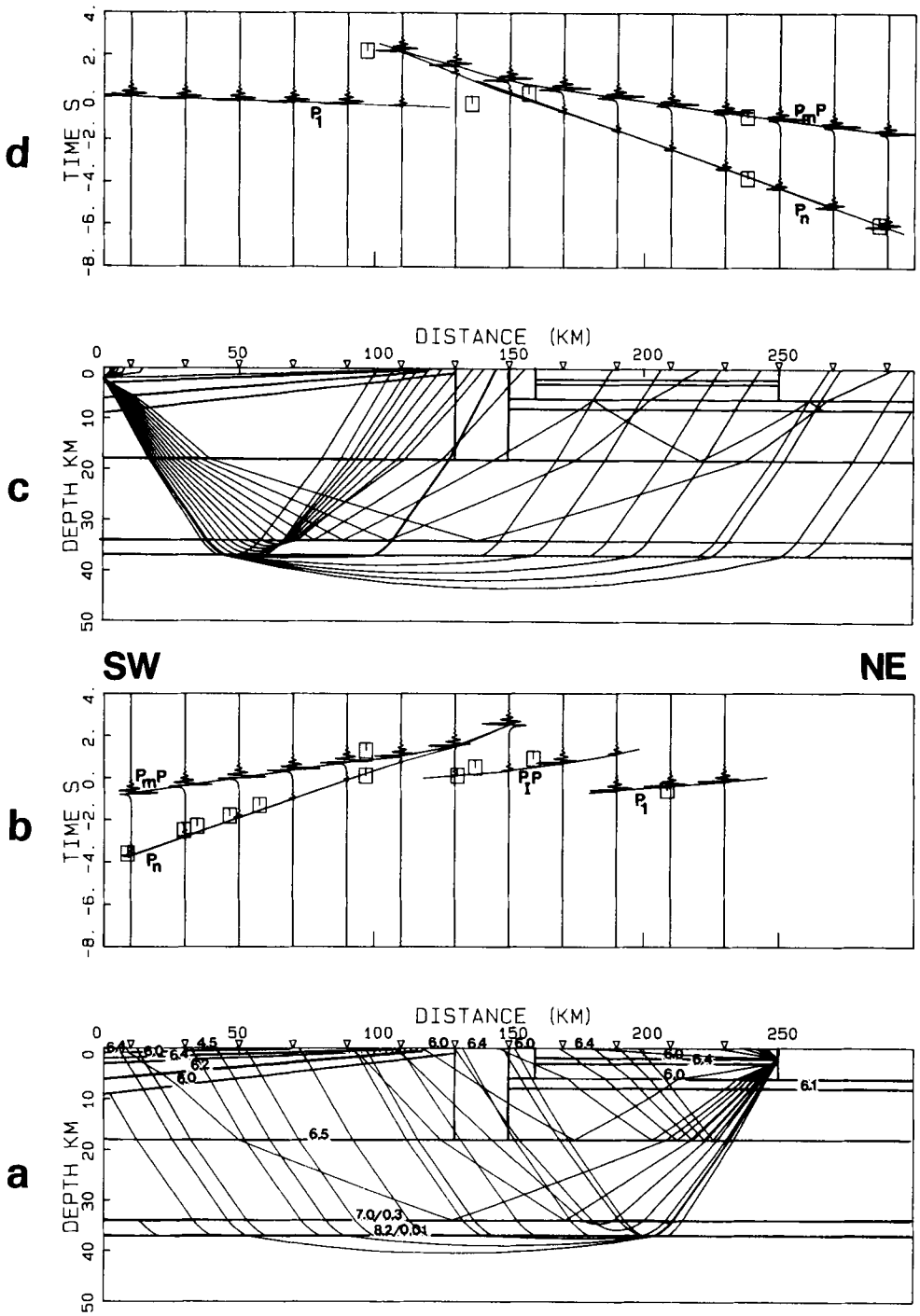

Figure 12. Velocity model, ray-trace diagram and synthetic record section for the OFS–East Rand–Witbank profile. Tremors from the (a) East Rand and (c) OFS goldfield. Reduction velocity 6 km s^{-1}.

and Witbank, and used to extend the OFS–East Rand profile to 320 km (Figs 2, 8). The crustal seismic velocity structure used to model the record sections observed on the OFS–East Rand profile is very similar to that used for the Klerksdorp–Witbank profile, with the exception of the Vredefort structure in the centre of the profile. The veloctiy structure within the Vredefort Dome is constrained by the detailed seismic refraction study of Green & Chetty (1990). The P_n phase is modelled by Moho at a depth of 36 km and an upper mantle velocity of 8.2 km s^{-1} (Fig. 12). The P_n and S_n curves, scaled assuming a Poisson's ratio of 0.25, match closely. A common Moho depth was used for both the *P*- and *S*-wave velocity models. In the vicinity of the East Rand the P_1P phase is modelled by an interface at a depth of 18 km. Correlation of the *S*-wave second arrivals (Figs 7b, 8b) proved difficult, and no satisfactory *S*-wave velocity model fitting both the forward and reversed profiles could be derived.

Poisson's ratio

We do not consider the *S*-wave velocity models obtained in this study sufficiently reliable to map Poisson's ratio through the crust. Nevertheless, our *S*-wave velocity models are comparable with the velocity–depth functions obtained by Bloch, Hales & Landisman (1969) for the northern

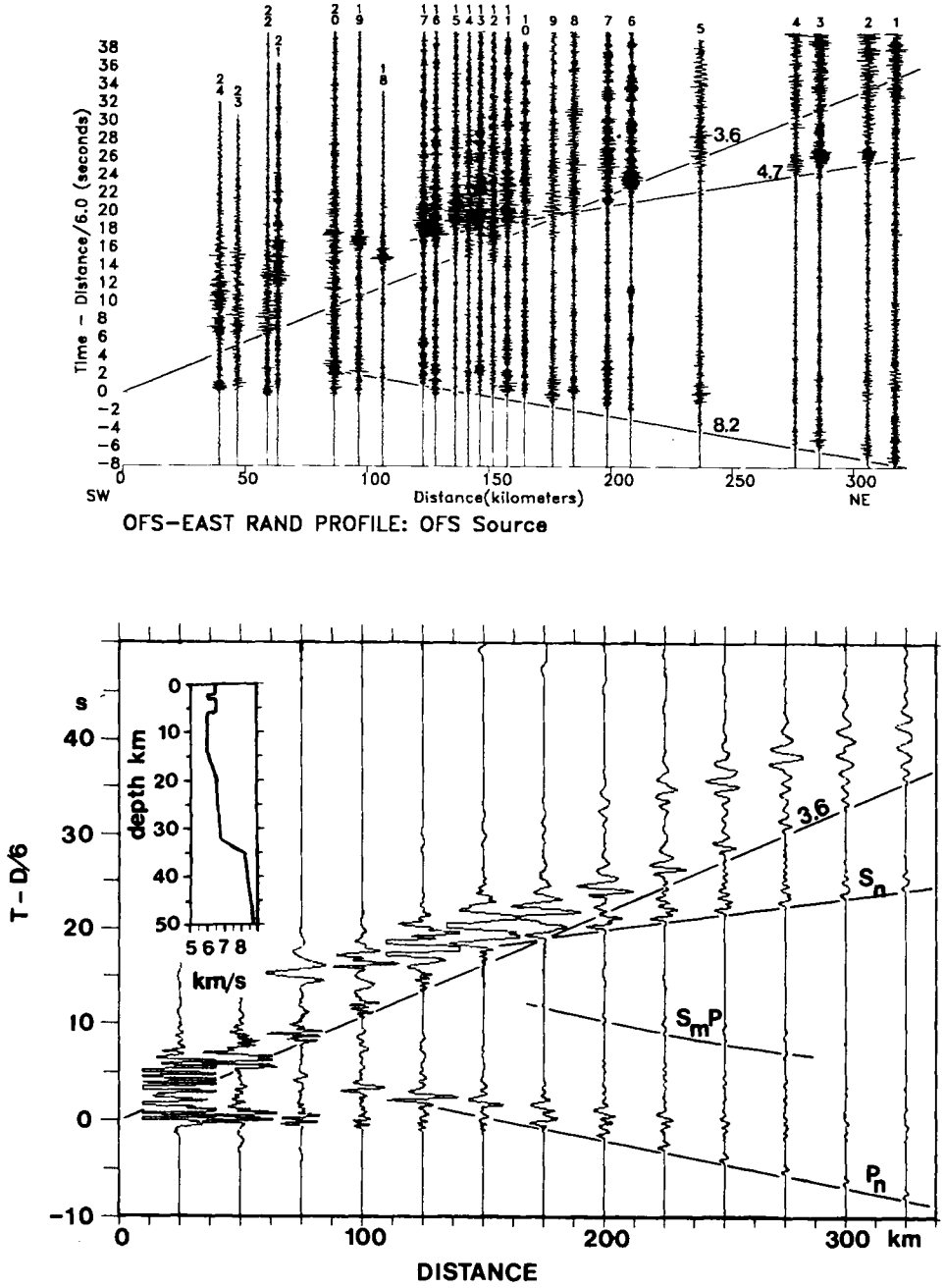

Figure 13. Synthetic record section for a generalized 1-D seismic velocity model of the central Kaapvaal Craton computed using the reflectivity method. The observed record section is for the OFS–East Rand profile. Reduction velocity 6 km s^{-1}.

Kaapvaal Craton by the inversion of the fundamental and first higher Rayleigh and Love modes. The *S*-wave velocity models for the Klerkdorp–Witbank profile show a zone with a relatively low *S*-wave velocity at the crust/mantle transition (Fig. 9c), and an *S*-wave velocity inversion in the lower crust (Fig. 11c), similar to that described by Bloch *et al.* (1969). In a comparison of the physical properties (*P*- and *S*-wave velocities, density, Poisson's ratio and conductivity) of the lower crust under Precambrian regions, Jones (1981) found that the Kaapvaal Craton differed from 'normal' and 'intermediate' crust by having a zone of high conductivity and relatively low *S*-wave velocity at the base of the crust. The v_P/v_S ratio for the lower crust of the northern Kaapvaal Craton is about 1.8 (Bloch *et al.* 1969), which corresponds to a Poisson's ratio of 0.28. These observations are compatible with serpentinization in the lower crust, provided the water of hydration does not escape (Jones 1981).

Reflectivity method modelling

The reflectivity method (Fuchs & Müller 1971) was used to calculate synthetic record sections for a generalized velocity model of the central Kaapvaal Craton. As the reflectivity method requires intensive computation it has not been attempted to model the details of the observed record sections. However, the main features have been successfully reproduced. *P*-wave velocities and *Q* values were assigned to each layer, and *S*-wave velocities calculated assuming a Poisson's ratio of 0.25. The density of each layer was calculated using the empirical density–velocity function of Birch (1964). Vertical component seismograms were calculated for 13 stations at 25 km intervals (Fig. 13). Each seismogram is 60 s in length and has a Nyquist frequency of 8.5 Hz. A dislocation point source (with a rise time of 0.05 s) was placed within a low-velocity layer in the upper crust, simulating a mine tremor with a focus within the Central Rand Group strata. The value of the L_g-wave *Q* within the Kaapvaal Craton has been measured to be 360 at 3 Hz (Frankel *et al.* 1990). A similar value was used for the crust in the reflectivity model. Each seismogram is normalized by the maximum amplitude on the first trace.

The *P*-wave velocity model and the vertical component synthetic record section are shown in Fig. 13 together with the record section for the OFS–East Rand profile. The synthetic record section shows a strong direct wave as the first arrival as far as 100 km. Beyond this a small-amplitude wave group with a phase velocity slightly higher than 6 km s^{-1} emerges as the first arrival. This is attributed to energy transmitted within the uppermost layer. Both the P_mP and S_mS phases give rise to large amplitude events just beyond the critical distance (100–120 km). The dominant frequency of these phases diminishes with offset due to the attenuating lower crust. A wave group, identified as the S_mP phase, emerges at a reduced traveltime of +10 s at an offset of 175 km. Its amplitude is considerably smaller than the P_mP phase. The sub-Moho velocity gradient ensures a strong P_n and S_n phase. Comparison with the observed data shows that the prominent phases are successfully reproduced by the generalized velocity–depth model.

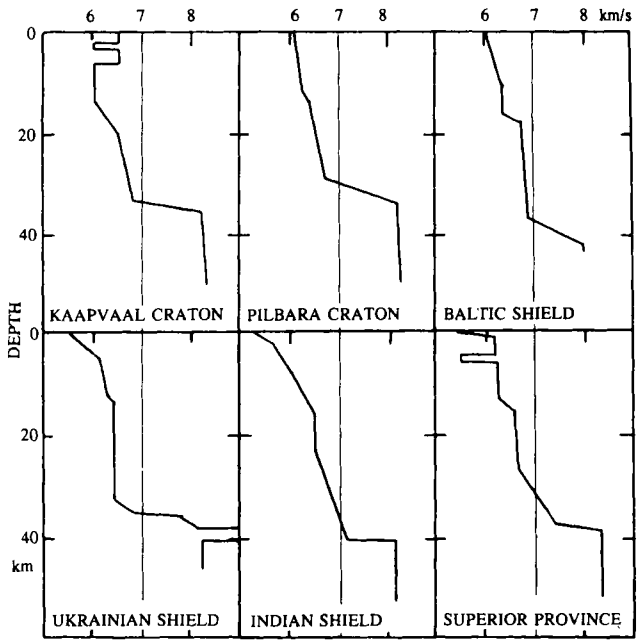

Figure 14. Velocity–depth models for the Archaean cratons (from this study and Drummond & Collins 1986).

DISCUSSION

Comparison with other Archaean cratons

The generalized *P*-wave velocity structure of the Kaapvaal Craton is compared with other Archaean cratons in Fig. 14. The Archaean cratons share the following features.

(a) An upper crystalline crust with seismic velocities in the range 6.2–6.4 km s^{-1}. Low-velocity zones are not commonly developed.

(b) The transition from upper to lower crust occurs at a depth which ranges from 12 to 18 km. It generally is marked by a velocity gradient rather than a first-order discontinuity.

(c) The lower crust has seismic velocities in the range 6.5–6.8 km s^{-1}. Velocities greater than 7 km s^{-1} are not frequently observed.

(d) The crust–mantle transition is generally a gradient zone 2–5 km thick over which the seismic velocity increases from about 6.8 km s^{-1} to about 8.1 km s^{-1}.

(e) The Moho is at a depth of 35 to 40 km.

Comparison with adjacent geological provinces

The *P*-wave velocity structure of the Kaapvaal Craton is compared with that of adjacent geological provinces (Fig. 1) in Fig. 15. The Archaean Limpopo Belt and Zimbabwe Craton lie to the north of the Kaapvaal Craton. The crustal thickness ranges from about 30 km in the centre of the Limpopo Belt to 40 km within the Zimbabwe Craton (Stuart & Zengeni 1987; Durrheim, Barker & Green 1991). These estimates of crustal thickness have been derived from observations of tremors at regional distances, timed blasts from open pit mines and gravity measurements. No detailed velocity–depth function is available.

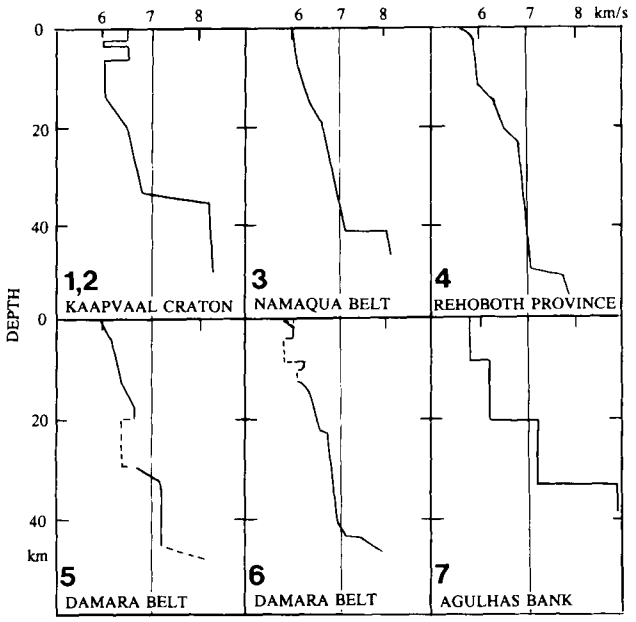

Figure 15. Velocity–depth models for southern Africa (from this study; Green & Durrheim 1990; Baier *et al.* 1983; Hales & Nation 1972). The numbers relate the velocity–depth models for the profile locations shown in Fig. 1.

The Kaapvaal Craton is rimmed to the south and southwest by the Proterozoic Namaqua Province. A seismic refraction investigation of the Namaqualand Metamorphic Complex (Green & Durrheim 1990) found that the lower crust is comprised of a substantial proportion of intermediate velocity (6.6–6.9 km s^{-1}) rocks with Moho at a depth of 42 km.

The Namaqua Province is in turn rimmed by the Pan-African (670–530 Ma) Damara province. A deep seismic sounding experiment was conducted in central Namibia by Baier *et al.* (1983). In the central zone of the Damara Orogen two velocity inversions are found in the upper crust; and the crust–mantle boundary is found to be a transition zone of variable width rising slightly from a depth of 47 km towards the Atlantic coast. The profile in the southern zone of the Orogen showed relatively high velocities (up to 6.6 km s^{-1}) in the upper and middle crust, and also in the lower crust (7.2 km s^{-1}). The profile in the Rehoboth Province (the basement rocks are concealed by cover strata, but are thought to be Proterozoic in age) to the south of the Orogen shows no velocity inversions in the upper crust; and Moho is split into an upper level at 47 km and a lower level at 60 km.

The basement rocks of the southern Cape are of the same age as the Damara Province. The region is also the locus of the most recent major tectonic event affecting southern Africa—the fragmentation of Gondwana (135–115 Ma). A seismic refraction survey on the continental shelf (the Agulhas Bank, described by Hales & Nation 1972) shows sediments extending to a depth of about 8 km; an upper crust with a velocity of 6.2 km s^{-1} extending to a depth of 21 km; a lower crust with a velocity of 7.2 km s^{-1}; and Moho at a depth of 33 km. The upper mantle has an unusually high seismic velocity of 8.95 km s^{-1}, but as the profile was unreversed the possibility of a dipping Moho cannot be excluded.

Implications for crustal evolution

The seismic velocity structure of the continental crust in southern Africa shows two important trends which should be taken into account in any model of crustal evolution. First, the Proterozoic crust is substantially thicker than the Archaean crust. Secondly, Proterozoic crust has a substantially thicker high-velocity (*P*-wave velocity > 7 km s^{-1}) lower crust. These trends were noted for the Precambrian crust of Australia (Drummond & Collins 1986; Drummond 1988), and have been confirmed by a world-wide review of seismic velocity–depth functions (Durrheim & Mooney 1991). We believe that these observations indicate that the primary crust building process in the Proterozoic differed from that in the Archaean. Seismic velocities in the range 7.0–7.6 km s^{-1} may indicate anorthosite or rocks of intermediate average composition in high-grade metamorphic facies, but the most common cause probably are rocks with a gabbro to olivine–gabbro bulk composition (Fountain & Christensen 1989). A thicker crust with a mafic basal layer can be produced in two ways. It can be formed by the shortening of an originally felsic crust, followed by igneous differentiation, uplift and erosion. However, Drummond & Collins (1986) demonstrate that vast amounts of tectonic thickening and erosion are required, and argue persuasively that basaltic underplating of the felsic crust is a more likely process. We seek to explain why Proterozoic, and not Archaean crust, is prone to basaltic underplating.

Several other important findings are pertinent to models of crustal evolution in southern Africa.

(a) The formation of diamonds requires high pressures and relatively low temperatures. The diamond stability field requires that the temperature at a depth of 150 km be less than 1075 °C (Kennedy & Kennedy 1986), a condition met by the present-day geotherm for the Kaapvaal Craton (Jones 1988). In southern Africa the diamond-bearing kimberlites are confined to the Archaean craton, while kimberlites in Proterozoic provinces are virtually barren (Gurney 1990). Further, many of the diamonds themselves are Archaean in age, even though the kimberlite eruptions may be much younger (Richardson *et al.* 1984). These results imply that the Kaapvaal Craton had already formed a substantial lithospheric keel by conductive cooling during the Archaean. This keel must be intrinsically less dense than the surrounding mantle in order to escape delamination as it cooled.

(b) Komatiitic volcanism is confined to the Archaean. The youngest komatiites in southern Africa are found in the 2.7 Ga Ventersdorp Supergroup (McIver, Cawthorn & Wyatt 1982). This indicates that mantle temperatures were significantly higher during the Archaean. Although preserved komatiitic lavas are now quite rare on the Kaapvaal craton, studies of the isotopic compositions of South African shales and greywackes indicate that the Archaean crust was composed of both granite (about 70 per cent) and a mafic

component (about 30 per cent) which could have been komatiite (Dia, Allègre & Erlank 1990).

(c) Isotopic studies have shown that the bulk of the continental crust of southern Africa differentiated from the mantle during the Archaean. Crust which stabilized during the Proterozoic is a mixture of recycled Archaean crustal material, and material separating from the mantle for the first time. The crust which stabilized during the Pan-African Damara orogeny consists entirely of recycled Archaean and Proterozoic crust (Harris *et al.* 1987).

Mantle temperature is considered to be the variable that controlled the transition from the Archaean to the Proterozoic type of crust (Durrheim & Mooney 1991). As the Earth cooled, the decrease in mantle temperature was sufficient to lead to a fundamental change in the crust-forming process. One possible mechanism is a change in the composition of magmatism (Jordan 1978; Hawkesworth *et al.* 1990). Hotter Archaean mantle temperatures led to the eruption of komatiitic lavas and the formation of a refractory lithosphere depleted in FeO, intrinsically less dense than the surrounding asthenosphere and thus not prone to delamination. Any underplated magma of komatiitic composition would be seismically indistinguishable from the mantle. The Archaean lithosphere stabilized and thickened by conductive cooling, enabling diamonds to be formed at depths exceeding 150 km. The depleted lithosphere was unable to produce an amount of basaltic melt to significantly intrude or underplate the Archaean crust during any subsequent heating event. As the mantle temperature decreased, komatiitic volcanism ceased and the Proterozoic crust formed above fertile mantle. Partial melting (instigated by plate subduction, rifting, or anorogenic heating) resulted in magmatic underplating by basalt (rather than komatiite) and crustal inflation, thereby thickening the Proterozoic crust and forming a high-velocity basal layer. This model (Fig. 16) is permissive of actualistic plate tectonic processes in the Archaean, but the magmatic products would include komatiite.

A similar mechanism has been used to explain a much more recent feature of African geology. Mid-plate volcanic rocks of Cainozoic age are concentrated in areas affected by Pan-African (*c.* 500 Ma) crustal reactivation, and virtually absent from cratonic areas. Ashwal & Burke (1989) interpret this to indicate that Pan-African areas are underlain by fertile mantle lithospheric mantle and cratons by depleted lithospheric mantle. Infertile mantle was delaminated from beneath areas thickened during continent–continent collision (especially during Pan-African times) and replaced by fertile mantle. Subsequent heating extracted magmas from the fertile but not the depleted mantle lithosphere.

CONCLUSIONS

This seismic refraction study has yielded a significantly more detailed and better constrained seismic velocity model of the central Kaapvaal Craton. It has the following features.

(a) Supracrustal strata are 0–10 km thick, with velocities of 3.5–6.8 km s^{-1}.

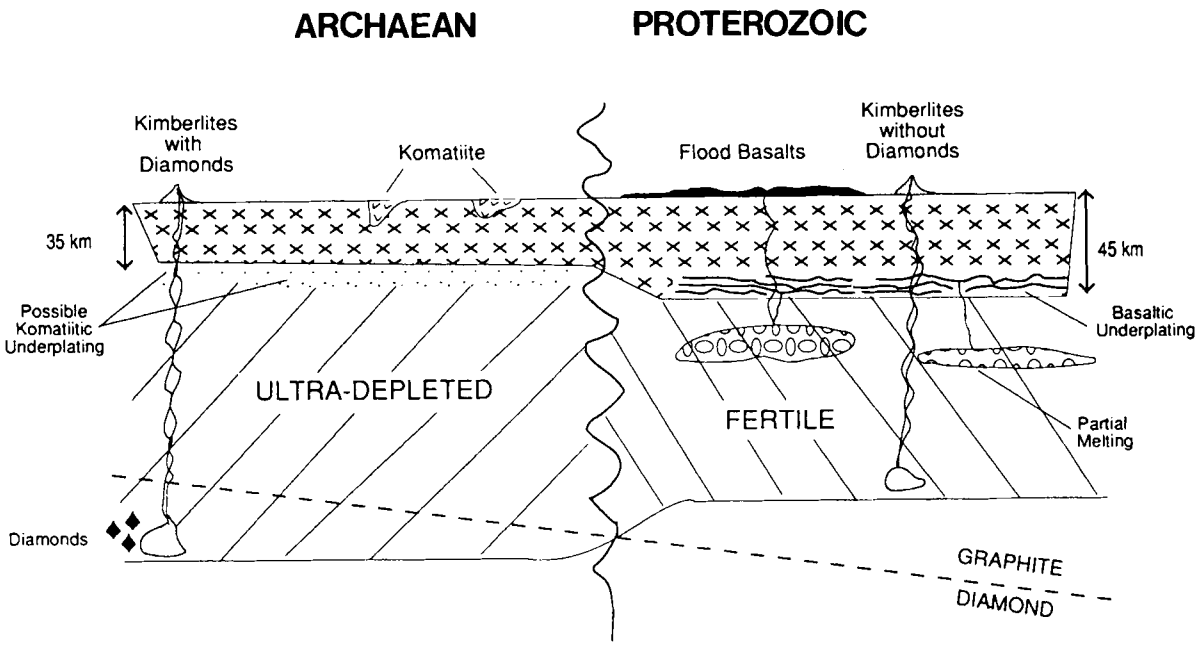

Figure 16. Model for Archaean and Proterozoic crustal evolution emphasizing differences in chemical properties of uppermost mantle (after Durrheim & Mooney 1991; based on the model proposed by Hawkesworth *et al.* 1990). Proterozoic crust develops above fertile (normal FeO) mantle that is the source of basaltic composition crustal underplating, leading to the development of thicker (45 km) crust. Archaean crust develops above initially hotter mantle that is depleted in FeO through the eruption of komatiitic lavas; magmatic underplating, if present, is ultramafic and is seismically indistinguishable from normal mantle. Presence of diamonds of Archaean age within kimberlites indicates that the lithosphere cooled and entered into the diamond stability field during the Archaean. The cold lithosopheric keel may also act as a thermal boundary against crustal underplating by basaltic melts from the asthenosphere.

(b) The upper part of the crystalline basement has a uniform velocity of 6.0–6.2 km s^{-1} with a thickness of about 10 km.

(c) The boundary between upper and lower crust is located at a depth of 12–18 km. It is sometimes marked by a velocity gradient, giving rise to a high-amplitude caustic at offsets of 150–180 km. In other areas the transition is sufficiently sharp for reflections to be generated.

(d) The lower crust has a rather uniform velocity in the range 6.4–6.7 km s^{-1}.

(e) The crust–mantle transition takes place over a distance of 1–3 km.

(f) The Moho is at a depth of about 35 km. A slight positive velocity gradient exists beneath the Moho.

(g) The crust has a relatively low value of Q revealed by the low dominant frequency of the supercritical Moho reflection, probably due to both anelastic absorption and scattering. The value of Poisson's ratio in the lower crust is about 0.28.

The petrology of the crystalline crust and upper mantle of the Kaapvaal Craton is deduced from a consideration of seismic velocities, Poisson's ratio, seismic attenuation, xenolith compositions, electrical conductivity, the Vredefort 'crust-on-edge' section and petrophysical data.

(a) The upper crystalline crust is composed of rocks with granitic to granodioritic average composition.

(b) The lower crust is composed of felsic granulite (no garnets) with a dioritic average composition.

(c) The crust–mantle transition is marked by a zone several kilometres thick, probably containing increasing amounts of serpentinized peridotite.

(d) The upper mantle consists predominantly of peridotite.

The velocity–depth model for the Kaapvaal Craton is essentially similar to models derived for other Archaean cratons. The Proterozoic provinces adjacent to the Kaapvaal craton are significantly thicker, and have an intermediate- to high-velocity layer developed at the base of the crust. This is interpreted to indicate a change in the process of crustal growth, with underplating becoming more important since the Archaean. This change is attributed to a change in the composition of the upper mantle. The higher temperatures in the Archaean mantle led to the eruption of komatiitic lavas, resulting in an ultradepleted mantle unable to produce significant volumes of basaltic melt. Proterozoic crust developed above fertile mantle, and subsequent partial melting resulted in basaltic underplating and crustal inflation.

ACKNOWLEDGMENTS

This project was funded by the South African National Geophysics Programme and the Chamber of Mines. M. Nkwana was responsible for much of the replaying and digitizing of the field tapes. P. Chipkin, M. Goldberg, A. Robertson and J. Sorour assisted in the maintenance of the seismographs. M. Muller computed the reflectivity method synthetic seismograms. We thank D. Gajewski (Technical University of Clausthal) for a useful and constructive review of the manuscript.

REFERENCES

Arnott, F. W., 1981. Seismicity in the Welkom area, O. F. S. (with special reference to the origin of the 1976-12-8 Event), *MSc dissertation*, University of the Witwatersrand.

Ashwal, L. D. & Burke, K., 1989. African lithosphere structure, volcanism, and topography, *Earth planet. Sci. Lett.*, **96,** 8–14.

Baier, B., Berckhemer, H., Gajewski, D., Green, R. W., Grimsel, Ch., Prodehl, C. & Vees, R., 1983. Deep seismic sounding in the area of the Damara Orogen, Namibia, in *Intracontinental Fold Belts*, pp. 887–900, eds Martin, H. & Eder, F. W., Springer-Verlag, Berlin.

Birch, F., 1964. Density and composition of the mantle and core. *J. geophys. Res.*, **69,** 4377–4387.

Bloch, S., Hales, A. L. & Landisman, M., 1969. Velocities in the crust and upper mantle of southern Africa from multi-mode surface wave dispersion, *Bull. seism. Soc. Am.*, **59,** 1599–1629.

Borchers, R., 1964. Exploration of the Witwatersrand system and its extensions, in *The Geology of some Ore Deposits in Southern Africa*, vol. 1, pp. 1–23, ed. Haughton, S. H., Geol. Soc. S. Afr., Johannesburg.

Braile, L. W. & Smith, R. B., 1975. Guide to the interpretation of crustal refraction profiles, *Geophys. J. R. astr. Soc.*, **40,** 145–176.

Brune, J. N., 1970. Tectonic stress and the spectra of seismic shear waves from earthquakes, *J. geophys. Res.*, **75,** 4997–5009.

Brune, J. N., 1971. Correction: Tectonic stress and the spectra of seismic shear waves from earthquakes, *J. geophys. Res.*, **76,** 5002.

Campbell, G. & Peace, D. G., 1984. Seismic reflection experiments for gold exploration, Wits. basin, Republic of South Africa, paper presented at the *46th Meeting of the European Association of Exploration Geophysicists*, London, 19–22 June 1984.

Carswell, D. A., Griffin, W. L. & Kresten, P., 1984. Peridotite nodules from the Ngopetseu and Lipelaneng kimberlites, Lesotho: a crustal or mantle origin?, in *Kimberlites II: the Mantle and Crust–Mantle Relationships*, pp. 229–243, ed. Kornprobst, J., Elsevier, Amsterdam.

Červený, V., Molotkov, I. A. & Pšenčík, I., 1977. *Ray Method in Seismology*, University of Karlova, Prague.

Cook, N. G. W., 1963. The seismic location of rockbursts, in *Proc. 5th Rock Mech. Symp.*, pp. 493–516, Pergamon, Oxford.

Dawson, J. B., 1980. *Kimberlites and their Xenoliths*, Springer-Verlag, Berlin.

Dawson, J. B. & Smith, J. V., 1987. Reduced sappharine granulite xenoliths from the Lace kimberlite, South Africa; implications for the deep structure of the Kaapvaal Craton, *Contrib. Mineral. Petrol.*, **95,** 376–383.

Dia, A., Allègre, C. J. & Erlank, A. J., 1990. The development of continental crust through geological time: the South African case, *Earth planet. Sci. Lett.*, **98,** 74–89.

Drummond, B. J., 1988. A review of crust/upper mantle structure in the Precambrian areas of Australia and implications for Precambrian crustal evolution, *Precambrian Res.*, **40/41,** 101–116.

Drummond, B. J. & Collins, C. D. N., 1986. Seismic evidence for underplating of the lower continental crust of Australia, *Earth planet. Sci. Lett.*, **79,** 361–372.

Durrheim, R. J. & Mooney, W. D., 1991. Archean and Proterozoic crustal evolution: evidence from crustal seismology, *Geology*, **19,** 606–609.

Durrheim, R. J., Barker, W. H. & Green, R. W. E., 1991. Seismic studies in the Limpopo belt, *Precambrian Res.*, in press.

Fernandez, L. M., Hyres, M., Graham, G., Ford, M., Nel, E., Moolman, A. C. & Molea, T., 1988. *Seismological Bulletin (May 1988)*, Report No. 1988-0136, Geological Survey of South Africa.

Fountain, D. & Christensen, N. I., 1989. Composition of the continental crust and upper mantle: A review, in *Geophysical Framework of the Continental United States,* pp. 711–742, eds Pakiser, L. C. & Mooney, W. D., Geological Society of America Memoir 172.

Frankel, A., McGarr, A., Bicknell, J., Mori, J., Seeber, L. & Cranswick, E., 1990. Attenuation of high-frequency shear waves in the crust: measurements from New York State, South Africa, and Southern California, *J. geophys. Res.*, **95,** 17 451–17 457.

Fuchs, K., 1975. Synthetic seismograms of PS-reflections from transition zones computed with the reflectivity method, *J. Geophys.*, **41,** 445–462.

Fuchs, K. & Müller, G., 1971. Computation of synthetic seismograms with the reflectivity method, *Geophys. J. R. astr. Soc.*, **23,** 417–433.

Gane, P. G., Atkins, A. R., Sellschop, J. P. F. & Seligman, P., 1956. Crustal structure in the Transvaal, *Bull. seism. Soc. Am.*, **46,** 293–316.

Gay, N. C., Spencer, D., Van Wyk, J. J. & Van den Heever, P. K., 1984. The control of geological and mining parameters on seismicity in the Klerksdorp gold mining district, in *Proc. 1st Int. Cong. on Rockbursts and Seismicity in Mines,* Johannesburg, 1984, pp. 107–120, eds Gay, N. C. & Wainwright, E. H., SAIMM, Johannesburg.

Gibson, B. S. & Levander, A. R., 1988. Lower crustal reflectivity in wide-angle seismic recordings, *Geophys. Res. Lett.*, **15,** 617–620.

Giese, P., 1976. Depth calculation, in *Explosion Seismology in Central Europe,* pp. 146–161, eds Giese, P., Prodehl, C. & Stein, A., Springer-Verlag, Berlin.

Green, R. W. E., 1973. A portable multi-channel seismic recorder and a data processing system, *Bull. seism. Soc. Am.*, **63,** 423–431.

Green, R. W. E. & Chetty, P., 1990. Seismic studies in the basement of the Vredefort structure, *Tectonophysics*, **171,** 105–113.

Green, R. W. E. & Durrheim, R. J., 1990. A seismic refraction investigation of the Namaqualand Metamorphic Complex, South Africa, *J. geophys. Res.*, **95,** 19 927–19 932.

Gurney, J. J., 1990. The diamondiferous roots of our wandering continent, *S. Afr. J. Geol.*, **93,** 424–437.

Hales, A. L. & Sacks, I. S., 1959. Evidence for an intermediate layer from crustal studies in the eastern Transvaal, *Geophys. J.*, **2,** 15–33.

Hales, A. L. & Nation, J. B., 1972. A crustal structure profile of the Agulhas Bank, *Bull. seism. Soc. Am.*, **62,** 1029–1051.

Harris, N. B. W., Hawkesworth, C. J., Van Calsteren, P. & McDermott, F., 1987. Evolution of continental crust in southern Africa, *Earth planet. Sci. Lett.*, **83,** 85–93.

Hart, R. J., Andreoli, M. A. G., Smith, C. B., Otter, M. L. & Durrheim, R. J., 1990. Ultramafic rocks in the centre of the Vredefort structure (South Africa): possible exposure of the upper mantle?, *Chem. Geol.*, **83,** 233–248.

Hartnady, C., Joubert, P. & Stowe, C., 1985. Proterozoic crustal evolution in southwestern Africa, *Episodes,* **8,** 236–244.

Hawkesworth, C. J., Kempton, P. D., Rogers, N. W., Ellam, R. M. & Van Calsteren, P. W., 1990. Continental mantle lithosphere, and shallow level enrichment processes in the Earth's mantle, *Earth planet. Sci. Lett.*, **96,** 256–268.

Holbrook, W. S., Gajewski, D., Krammer, A. & Prodehl, C., 1988. An interpretation of wide-angle compresssional and shear wave data in southwest Germany: Poisson's ratio and petrological implications, *J. geophys. Res.*, **93,** 12 081–12.106.

Jones, A. G., 1981. On a type classification of lower crustal layers under Precambrian regions, *J. Geophys.*, **49,** 226–233.

Jones, M. Q. W., 1988. Heat flow in the Witwatersrand and environs and its significance for the South African shield geotherm and lithosphere thickness, *J. geophys. Res.*, **93,** 3243–3260.

Jordan, T. H., 1978. Composition and development of the continental tectosphere, *Nature,* **274,** 544–548.

Kasahara, K., 1981. *Earthquake Mechanics,* Cambridge Earth Science Series, Cambridge University Press, Cambridge, UK.

Kennedy, C. S. & Kennedy, G. C., 1976. The equilibrium boundary between graphite and diamond, *J. geophys. Res.*, **81,** 2467–2470.

McGarr, A., 1976. Seismic moments and volume changes, *J. geophys. Res.*, **81,** 1487–1494.

McIver, J. R., Cawthorn, R. G. & Wyatt, B. A., 1982. The Ventersdorp Supergroup—the youngest komatiitic sequence in South Africa, in *Komatiites,* pp. 81–90, eds Arndt, N. T. & Nisbet, E. G., George Allen & Unwin, London.

Mitchell, B. J., Yacoub, N. K. & Correig, A. M., 1977. A summary of seismic surface wave attenuation and its regional variation across continents and oceans, in *The Earth's Crust,* Am. Geophys. Union Monogr., vol. 20, pp. 723–724, ed. Heacock, J. G., Am. Geophys. Un., Washington, DC.

Mooney, W. D. & Prodehl, C. (eds), 1984. *Proceedings of the 1980 Workshop of the International Association of Seismology and Physics of the Earth's Interior on the Seismic Modeling of Laterally Varying Structures: Contributions Based on Data from the 1978 Saudi Arabian Refraction Profile,* US Geol. Surv. Circ. 937, Alexandria, VA.

Nicolaysen, L. O., 1990. The Vredefort structure: an introduction and a guide to recent literature, *Tectonophysics,* **171,** 1–6.

Nixon, P. H., 1987. Kimberlite xenoliths and their cratonic setting, in *Mantle Xenoliths,* pp. 215–240, ed. Nixon, P. H., John Wiley & Sons, Chichester.

Percival, J. A. & Berry, M. J., 1987. The lower crust of the continents, in *Composition, Structure and Dynamics of the Lithosphere–Asthenosphere System,* pp. 33–60, eds Fuchs, K. & Froidevaux, C., Geodynamics Series, vol. 16, American Geophysical Union, Washington, DC.

Potgieter, G. J. & Roering, C., 1984. The influence of geology on the mechanisms of mining-induced seismicity in the Klerksdorp goldfield, in *Proc. 1st Int. Cong. on Rockbursts and Seismicity in Mines,* pp. 45–50, eds Gay, N. C. & Wainwright, E. H., SAIMM, Johannesburg.

Pretorius, C. C., Jamison, A. A. & Irons, C., 1989. Seismic exploration in the Witwatersrand basin, Republic of South Africa, in *Proceedings of Exploration '87: Third Decennial International Conference on Geophysical and Geochemical Exploration for Minerals and Groundwater,* pp. 241–253, ed. Garland, G. D., Spec. vol. 3, Ontario Geol. Survey.

Raynaud, B., 1988. The quantitative interpretation of deep seismic reflection data, *First Break,* **6,** 223–231.

Richards, P. G. & Menke, W., 1983. The apparent attenuation of a scattering medium, *Bull. seism. Soc. Am.*, **73,** 1005–1021.

Richardson, S. H., Gurney, J. H., Erlank, A. J. & Harris, J. W., 1984. Origin of diamonds in old enriched mantle, *Nature,* **310,** 198–202.

Roux, A. T., 1970. The application of geophysics to gold exploration in South Africa, in *Mining and Groundwater Geophysics/1967,* pp. 425–438, ed. Morley, L. W., Econ. Geol. Rep. 26, Geol. Surv. Canada.

Schoenberger, M. & Levin, F. K., 1974. Apparent attenuation due to intrabed multiplies, *Geophysics,* **39,** 278–291.

Shapira, A., 1988. Rg waves from rockbursts in South Africa, *Tectonophysics,* **156,** 267–273.

Slichter, L. B., 1932. The theory of the interpretation of seismic travel time curves in horizontal structures, *Physics,* **3,** 273–295.

Spence, G. D., Whittall, K. P. & Clowes, R. M., 1984. Practical synthetic seismograms for laterally varying media calculated by asymptotic ray theory, *Bull. seism. Soc. Am.*, **74,** 1209–1223.

Spottiswoode, S. M. & McGarr, A., 1975. Source parameters of tremors in a deep-level gold mine, *Bull. seism. Soc. Am.*, **65,** 93–112.

Stepto, D., 1979. A geological and geophysical study of the central portion of the Vredefort dome structure, *PhD thesis,* University of the Witwatersrand.

Stuart, G. W. & Zengeni, T. G., 1987. Seismic crustal structure of the Limpopo mobile belt, Zimbabwe, *Tectonophysics,* **144,** 323–335.

Tankard, A. J., Jackson, M. P. A., Eriksson, K. A., Hobday, D. K., Hunter, D. R. & Minter, W. E. L., 1982. *Crustal Evolution of Southern Africa. 3.8 Billion Years of Earth History,* Springer-Verlag, New York.

Tittman, B. R., 1977. Internal friction measurements and their implications in seismic Q structure models of the crust, in *The Earth's Crust,* Am. Geophys. Union Monogr., vol. 20, pp. 197–213, ed. Heacock, J. G., Am Geophys. Un., Washington, DC.

Toksöz, M. N. & Johnston, J. H. (eds), 1981. *Seismic Wave Attenuation,* Soc. Expl. Geophys., Tulsa, OK.

Van Calsteren, P. C. W., Harris, N. B. W., Hawkesworth, C. J., Menzies, M. A. & Rogers, N. W., 1986. Xenoliths from southern Africa: a perspective on the lower crust, in *The Nature of the Lower Crust,* pp. 351–362, eds Dawson, J. B., Carswell, D. A., Hall, J. & Wedepohl, K. H., Geological Society Special Publication No. 24, London.

Van Zijl, J. S. V., 1978. The relationship between the deep electrical structure and tectonic provinces in southern Africa. Part 1. Results obtained by Schlumberger soundings, *Trans. geol. S. Afr.*, **81,** 129–142.

Walraven, F., Armstrong, R. A. & Kruger, F. J., 1990. A chronostratigraphic framework for the north-central Kaapvaal craton, the Bushveld Complex and the Vredefort structure, *Tectonophysics,* **171,** 23–48.

Weder, E. E. W., 1990. The significance of gravity and seismic reflection techniques in deriving a new structural model for the areas south of the Central Rand goldfields, *PhD thesis,* University of Pretoria.

Willmore, P. L., Hales, A. L. & Gane, P. G., 1952. A seismic investigation of crustal structure in the western Transvaal, *Bull. seism. Soc. Am.*, **42,** 53–80.

Wu, R. S. & Aki, K., 1985. Elastic wave scattering by a random medium and the small scale inhomogeneities in the lithosphere, *J. geophys. Res.*, **90,** 10 261–10 273.